# GEOLOGICAL INVESTIGATIONS AND QUALITY ASSESSMENT OF TOUNGO GRAPHITE, NORTHEASTERN NIGERIA

**BY**

**ZIRA, DLAMA KAMAUNJI**

**M.Sc/GL/05/395**

**A Thesis Submitted to the School of Postgraduate Studies, Federal University of Technology, Yola, in Partial Fulfilment of the Requirement for the award of M.Sc Degree in Mineral Exploration**

**AUGUST, 2011**

## DECLARATION

This is to certify that I, Mr. Dlama Kamaunji Zira, a Masters Degree Student in the Department of Geology with registration no. M.Sc/GL/05/395 has satisfactorily completed the research project works for M.Sc in Mineral Exploration. The work embedded in this research project is original and has not been submitted in part or in full for any other degree or certificate to this or any other university.

Signed:

.....

Dlama K. Zira

**APPROVAL PAGE**

## DEDICATION

This work is dedicated to geologists and other earth scientists alike without whom the riches of the earth's mineral kingdom would not have been explored.

## ACKNOWLEDGEMENT

This work could not have seen the light of day without the immense assistance of the following to whom I acknowledge my gratitude and indebtedness: Prof. A. Nur, Prof. Eyo E. Ntekim (my supervisor), Dr. Jackson Ishaku, N. Bassey, Mamman Dabari, V.I Haruna and all other lecturers and staff members of Geology Department for the invaluable assistance and understanding during the period of study; to Mal. Jamil Baba, Yakubu Muhammed, Obi Nwosu, Oluwolafe Yemi and Abdullahi Ibrahim Tumu, staff of the Nigerian Metallurgical Development Center (NMDC), Jos for carrying out detailed chemical, determinative and metallurgical tests on graphite samples; to Idoko Agada, Lecturer, Department of Geology, University of Jos and Mr. Chollom Gyang, Assist. Chief Laboratory Technologist for thin section study, to Mr. Isa Oga Angulu, Dept. Of Physics, Experimental Records also of the University of Jos, for thermal conductivity and electrical resistivity tests on graphite samples; to Dr. Kameel, Chief Scientist, Aston Microscopy and Engineering, Aston University, UK, for chemical analysis on all the rock samples, to Mr. L.B. Ryan, Principal Partner, West African Minerals, UK, for all-round support and assistance for chemical analysis test while in the UK; to Mr. Asanarimam Chimbekujwo and my son V. D. Kamaunji, for computer works and lastly but not the least, to Adamawa State Government for sponsorship. To God, I say hallelujah, for everything.

## TABLE OF CONTENT

## LIST OF FIGURES

## LIST OF TABLES

## LIST OF PLATES

## APPENDICES

## ABSTRACT

Flake graphite deposit occurs within the Precambrian rocks of Toungo area in northeastern Nigeria. Detailed field and laboratory investigations show that the oldest rocks in the area are migmatite gneisses and the Pan African granites which evolved through progressive regional metamorphism and granite intrusion during the different tectonic episodes. These rock units form components of the Nigerian Basement Complex rocks. The graphitic rocks in the area are hosted by amphibolites which were affected by the upper amphibole facies metamorphism during the Pan African orogeny. Results of physical, chemical, metallurgical and consumer tests on the Toungo graphite with different standard equipment conform to internationally accepted quality standards for industrial utilization. The excellent thermal shock resistance of the graphite indicates the high thermal shock required by most commercial refractories worldwide. The high thermal conductivity of the graphite is an indication of their suitability for specification acceptance, heat loss estimation, surface temperature and design for construction of refractories. The light weight shown by results of bulk density with low thermal expansion would make these materials less susceptible to expansion while their inertness shown by none-reaction with nitric acid implies their usability in high corrosive environments. The high electrical resistance and thermal conductivities also confer high thermal shock to the material, an advantage in electrical fields and aerospace industries. The carbon contents of the graphite can be enhanced by upgrading through beneficiation process. The data obtained in almost all the tests are quite satisfactory and meet international quality standards of graphite for industrial utilization.


## CHAPTER ONE

# INTRODUCTION

Reconnaissance Mineral Resources Surveys of Toungo area in the Northeast region of Nigeria was carried out as part of an appraisal programme towards documentation of the vast solid mineral resources of the area (Ministry of Commerce and Solid Minerals, Yola, 2004). The survey programme covered Mbulo, Yebbi, Gurampawo, Ngandu, Kiri, Kogin Baba, Labare, Bayan Dutse, Nalomi, Disigba, Koncha, Jangani, Dau, Mayo Butale and Mayo Chacha areas. This followed a publication by the Geological Survey of Nigeria (GSN, 1987) which showed existence of a number of mineral resources, including the occurrences of graphite in Hosere Nuwa, Gayam, Jauro Jalo and Mayo Butale in Toungo area.

The principal objective of the initial study was to produce an inventory of mineral deposits in the area. With the assistance of Toungo Local Government Council, the District Heads of Toungo, Kiri, Yebbi and Dau Districts, the Vigilante Group and Regional Geological Maps (1:250, 000) prepared by Consulint Nig. Ltd; (1976), two sites where exploration trenches were dug by the British were located at Mayo Nyanyare (about 6km S.W of Mayo Butale) and Walon Kole valley (about 5km N.W of Mayo Butale and about 11km South of Toungo Town) (Fig. 1a).

## 1.1 NATURAL CHARACTERISTICS

### 1.1.1 Location and Accessibility

The area under study is located in Toungo Local Government Area within Nigerian 1:50, 000 topographical sheets Kiri 237 S.E and Dau 257 N.E. It is situated between latitudes

Fig. 1a: Map of Toungo Area showing the Project area

8 ° 10' 00" N and longitudes 11° 57' 00" - 12° 00' 00" E. The area is accessible by Trunk ‘A’ Yola – Ganye – Toungo Federal road and is about 215km from Yola (Fig. 1b). It borders the

Gumti – Gashaka National Park to the East and South – East, Kiri mountain ranges to the West and Toungo town to the North.

### 1.1.2 The Physical Setting

The project area has two major definable relief zones and these are:

a. The peneplains which range from 450 – 750 meters above sea level. These correspond to the seemingly low-lying areas, rivers valleys and flood plains. They are gently undulating and some have been dissected by strong erosive river courses.
b. The hills and highlands form the second group and these range from about 751 to more than 2, 000 meters above sea level. These highlands form part of Shebshi Mountain ranges which are major watersheds in the Southern part of Adamawa State. Other Mountain ranges in the zone include the Mandara, Alantika and the Adamawa highlands which trend NE – SW, forming part of the Cameroun volcanic line. These highlands also form part of the highest mountain ranges in the country where Chabal Nodi, 2420 meters above sea level, is highest in Nigeria.

The project area lies wholly within the highlands and near the Vogel peak, which is about 2045 meters above sea level (and of course the highest in Adamawa State). The highest peak in the project area is in the north-central part and is about 800 meters above sea level while the lowest is 550 meters and is found in Mayo Butale valley in the south eastern part of the area. The main rivers that drain the area include Mayo Butale, Jerendi and Mayo Walon Kole.

Fig 1b: Location of the Project site

### 1.1.3 Climate, Vegetation and Soils

Climatically, the area belongs to the tropical hinterland and falls within the southern Guinea climatological zone. According to Dar Alhandah and Partners (1978) and Sotesa (1979), the zone has the following climatic characteristics:

a. Climatic type: Tropical wet and dry seasons (Wet season: March/April – October; dry season: November – March).
b. Mean Annual rainfall 700 – 1200mm
c. Elevation, in meters above sea level: 500 – 2, 000 meters
d. Aridity index: 1.6
e. Mean Annual Temperature: 24 - 27°C

The natural vegetation belongs to the tropical grassland and is characterized by the Southern Guinea Savanna which consists of undifferentiated woodland savanna systems. The vegetation cover is thick with mixtures of short and tall grasses and trees forming dry forests in some areas, (Plate 1) (Darl-al-Handasah and Partners, 1978). Rivers and streams found in the area are mostly seasonal and form trellised drainage network, flowing from high points in the west, north – west and south – south – east wards to the Gumti National Park in the east. (Fig. 1).

The main soil type found in the area is the ferruginous tropical soil. There are also the weakly developed soils, which are associated with sloppy or hilly areas with good drainage systems.

Plate 1: Natural Vegetation of the project area

### 1.2.4 Geological Setting of the Study Area

The Nigerian basement complex consists of Precambrian migmatitic suites, older and newer metasediments and Pan African granites, and Cenozoic volcanic rocks. The migmatite suite is made up of gneisses and migmatites and is believed to have been formed during the Eburnean Orogeny (Grant, 1969; Rahaman, 1981; Woakes *et al*, 1987). However, recent studies from radiometric data on the basement rocks by Dada *et al* (1993); Briquier *et al* (1994); Ekwueme and Kroner (1997, 2000); indicate that the migmatitic – gneiss – quartzite complex dates back to Archaean ages of 3560 – 3000 Ma (Rahaman, 2003). In the project area, the migmatitic – gneiss – quartzite complex are located in the northwestern part of the area and are strike-slip faulted along NW – SE and NE – SW axis.

The Pan African granites in Nigeria evolved during the Pan African thermotectonic period by uplift, cooling, fractionation, faulting and high-level magmatic activity which resulted into granite intrusion and orogenesis (McCurry, 1976). In the area of study, the Pan African granites occupy about two-third of the project area, and they seem to enclose the migmatite – gneiss – quartzite complex. They are mostly located to the south and north – central portion of the area. The granites have been identified as biotite granites, pegmatitic granites, granite gneisses and amphibolites. According to Rahaman (2003), the project area (and environs) form part of a rectangular block broken into three (3) zones on the eastern border of Nigeria with Cameroun Republic and a component of polycyclic migmatite – gneiss – quartzite complex intruded by Pan African granites during the Pan African Orogeny, 600±150 Ma. Volcanic rocks, found to the north and north – eastern parts of the area are due to high level volcanic activity in the area during the Cenozoic (McCurry, 1976).

The youngest deposits in the area include eluvium and the alluvial complexes. The eluvium is the weathered portion of the Precambrian basement and is mostly lateritic (Plate 2), while the alluvial complexes form old and young alluvium. The old alluvium is made up of silts, sands, silty clays, pebbles and colluviums. The young alluvium is characterized by sands, silts, clays, and gravels and found along flood plains in the area. Geochronological record of the rock units are given in Table 1 while a probable sequence of events in the area is given in Table 2.

In the project area, graphite outcrops in two main locations: the first site is at Walon Kole village, northeastern part of the area while the second outcrop is in the southwest, near Mayo Butale village (Fig. 2). They are mainly hosted by amphibolites which in turn are bounded by pyroxenites, gneisses, migmatites and migmatitic gneisses in the west, south – west and north – west respectively (Fig 3). The amphibolites form part of the Pan African granites in the area and must have evolved through deformation, metamorphism, reactivation and isostatic readjustment of pre-existing rocks during the Pan African Orogeny (Rahaman, 1981). The amphibolites form a group of rocks composed mainly of amphiboles and plagioclase feldspars with little or no quartz (Wikipedia, 2010). They are typically dark coloured and heavy, with a weakly foliated or schistose (flaky) structure.

## 1.2 THE HUMAN ENVIRONMENT

The inhabitants of Toungo Local Government Area include the Chambas (who are the original indigenes) and other settlers like the Mumuyes, Fulanis, Hausa, Tivs and people from the neighbouring Cameroun Republic. The population of Toungo area is 68, 615 (National Population Commission, Adamawa State, 2011). The people live in segmented large and small

Plate 2

## TABLE 1: PROBABLE GEOLOGICAL SEQUENCE OF EVENTS OF THE ROCK UNITS IN THE PROJECT AREA AND ENVIRONS

| Age | Geological Episode/Tectonic activity | Petrogenetic unit | Rock type |
|---|---|---|---|
| Quaternary to recent sediments | Disintegration of uplifted areas by various petrogenetic modes such as biochemical, endogenetic and volcanic processes by mechanical, physical and chemical weathering. | Quaternary to recent sediments | Alluvium, Alluvium |
| Cenozoic volcanic rocks 60±70 myrs | Extrusion of basalt flows and cones and volcanic plugs which is related to Cameroun volcanic line and Gulf of Guinea volcanism. | Olivine basalt flows and cones | Basalts and basaltic flows |
| Lower Paleozoic to pre-Cambrian Pan African granites 650±150 myrs | Uplift, cooling, fractionation, faulting, high-level magnetic activity, granite intrusion, orogenesis, deformation, metamorphism, reactivation and isostatic readjustment of pre-existing rocks | Fine-med grained biotite granites, granite-gneiss, pegmatitic granites, amphibolites | Biotite granites, pegmatitic biotite granites, granite-gneisses and amphibolites |
| Pre-Cambrian Eburnean granites 2.8 ± 300 myrs | Intense deformation, isoclinal folding, progressive regional metamorphism, migmatisation, formation of banded gneiss at Gudaru granitization thru at least 2 tectono-metamorphic cycles | Migmatities, migmatitic granites, gneisses, schists | Migmatities, granites, gneisses and schists. |
| Pre-Cambrian Basement >3000myrs | | Undifferentiated basement complex rocks such as migmatitic granites, gneisses, schists | Weathered Precambrian basement |

**TABLE 2: GEOCHRONOLOGY OF ROCK UNITS IN THE PROJECT AREA AND ENVIRONS**

| Epoch/Age | Rock type | Petrogenetic units |
|---|---|---|
| Quaternary to recent sediments | Quaternary to recent sediments | Alluvium, Eluvium |
| Cenozoic volcanic rocks, 60±70 ma | Cenozoic Volcanics | Basalts and basaltic flows |
| Lower Paleozoic to pre-Cambrian: 650±150 ma | Pan African Granites | Biotite granites, pegmatitic biotite granites, granite-gneisses and amphiboles |
| Proterozoic (Upper) 2000 ± 300 ma | Eburnean granites | Migmatites, migmatitic granites, gneisses and schists |
| Late Archaean, 2800 – 2500 ma | Liberian/Dahomean | Migmatites, granites, gneisses, gneisses and schists. |
| Early Archaean, 3, 500 – 3, 000 ma | Liberian/Dahomean, Early gneiss | Early gneisses (?) granite – gneiss, pyroxene, gneisses (?) |

*After McCurry and Wright (1971)*

Fig 2 Satellite Imagery of the project area

Fig 3 General Geology if the project area

communities and with a population density of about 11 people per square kilometer; it is one of the least populated Local Government Areas in Adamawa State. However, Toungo town (which is the headquarters of the Local Government Area has the highest population density). In terms of occupation, the primary economic activity of the people is agriculture in which 80 – 85% of the entire active population is involved. Crops grown include yams, maize, rice, guinea corn, sugar cane, cocoa, groundnut and fruits such as mangoes, bananas, guavas, oranges, cassava and vegetables. Secondary economic activities are mostly commercially based and include block making, petty trading, metal and mechanical works, carpentry, small scale mining, welding, grinding, baking, building construction, cattle rearing, hunting, tailoring and shoes and leather works in which about 10% of the population are involved. Civil servant form about 5% of the population.

## 1.3 STATEMENT OF THE PROBLEM

Despite the reported occurrences of graphite in the study area by the Geological Survey of Nigeria (GSN, 1987) and the discovered earlier exploration by the colonial regime in 1948, no effort has been made to assess the extent of neither graphite mineralization nor its industrial suitability.

## 1.4 AIMS AND OBJECTIVES

### 1.4.1 Aims

This research project aims at carrying out determinative tests in addition to field investigations in order to appraise appropriate use of the Toungo graphite.

### 1.4.2 Objectives

The objectives of this work are four-fold, namely:

a. To carry out geological mapping of the area within coordinates 11° 57' 00" - 12° 00' 00" East and 7° 57' 30" – 8° 01' 00" North, on a scale of 1:26, 000;
b. To find out from the field studies and determinative physico – chemical tests, the type of graphite bodies existent in the area;
c. To assess the industrial application of the graphite by carrying out field and laboratory studies such as physical, chemical and determinative tests on the graphite including metallurgical and consumer tests; and
d. On the basis of field and laboratory studies, attempt will be made to establish the geological history, origin and evolutionary trend of rocks in the area.

## 1.5 SCOPE OF THE STUDY

The study involved geological mapping and sampling of rocks of the project area. The rocks were subjected to physical and determinative tests in the field and detailed laboratory studies in respect of metallurgical, consumer and chemical tests.

## 1.6 LIMITATION

To assess the industrial potentials of Toungo graphite, field samples were collected from only the two identified mineralized areas.

# CHAPTER TWO

# LITERATURE REVIEW

## 2.1 PROPERTIES OF GRAPHITE

Graphite is one of the two allotropes of natural crystalline carbon; the other is diamond. The exotic forms of crystalline carbon include carbon nanofibers and fullerens (Wikipedia, 2008; Olson, 2009). Graphite holds the distinction as the highest stable form of carbon compound that is not attacked by acids and not used as fuel due to its inability to ignite (Wikipedia, 2008). It derives its name from the Greek word 'Graphein', meaning to draw/write (as used by Abraham Gottob Werner in 1789), for its use in pencils, (Wikipedia, 2011b). Graphene is a one atom thick planar sheet of $sp^2$ bonded carbon atoms which are densely packed in a honey-comb crystal lattice. It is known to be the strongest material in the world and can be viewed as atomic-scale chicken wires made from carbon atoms and their bonds" (Wikipedia, 2008). It is the basic structural element of all other graphite materials such as graphite itself, carbon nanofibers and fullerenes (Wikipedia, 2008; Lueking *et al*, 2005) (Fig 4a).

Graphite has a density of 1.9 – 2.3, a metallic luster and lustrous black sheen, and is grayish black or opaque in colour (Mitchell, 1993; Wikipedia, 2008; Olson, 2009). It has high thermal and electrical conductivity; is highly refractive and chemically inert; has low absorption of X-ray and neutrons due to low hardness. The thin flakes of graphite are flexible but not elastic (Wikipedia, 2008; Olson, 2009). It is extremely soft due to its low hardness (1 – 2 on Mohr's scale); feels greasy or slippery to touch and colours anything black (Fig. 4b) that comes in slight

Fig 4 a and b

contact with it (Elert, 2004; Microsoft Encarta, 2009). These distinguishing characteristics of graphite are due to graphite's crystal structure (Hurlbut and Klein, 1971), as shown in Fig. 5 (A – C). The carbon atoms assume a hexagonal structural arrangement in planar fashion and are covalently bonded within the rings (Fig. 5D) while the layers are stacked parallel to each other and held loosely by Van Der Waals forces (Ceram Research, 2006). Graphite has high degree of anisotropy due to the two types of bonding which act in different crystallographic directions due to its metallic and non-metallic properties (Wikipedia, 2008).

### 2.1.1 Geological Setting of Graphite

The geological setting and depositional environment of graphite is usually metasedimentary belts of granulite or upper amphibolite facies metamorphism which have been invaded by igneous rocks (Simandi and Kenan, 1997). The metamorphic rocks of these terrains play host to graphite deposits and these include gneisses, paragneisses, quartzite, marbles, iron formations, amphibolites, pegmatites, orthogneisses, charnockites, and granulites (Simandi and Kenan, 1997). Other host rocks include quartz-mica schists, feldspathic or micaceous quartzite and gneisses, and metamorphic carbonaceous rocks (Mitchell, 1993). Mitchell (1993) also pointed out that economic deposits of graphite are associated with Achaean or late Proterozoic rocks and may contain up to 90%, graphite but typical grade range between 10 – 15% graphite.

Most graphite deposits are usually strata-bound with lenses ranging from 30cm to 30m thick, but could extend up to 2km (Mitchell, 1993). The ore bodies are usually tabular or lenticular and occur as irregular bodies especially in the hinge zone of folds. Studies have shown that low grade deposits are hosted by paragneisses and are stratabounds, while high grade

Fig 5 (a and b)

Plate 5 (c, d)

deposits are associated with fold crest along the paragneisses-marble, quartzite-marble and quartzite-paragneisses contacts or located along other zones that acted as channels for retrograde metamorphism (Mitchell, 1993). In such rock units or contact zones the possible geochemical indicators used to detect graphite anomalies during geochemical exploration include positive vanadium and nickel and negative boron, and appreciable sulphides and uranium contents (Mitchell, 1993). Impurities or gange mineral include sedimentary minerals such as quartz, feldspar, mica, amphibole, garnet, calcite, pyrrhotite, pyrite and magnetite. Others include biotite, with or without clinopyroxenes kyanite, clinozoisite, scapolites, sulphur and gypsum (Simandi and Kenan, 1997).

### 2.1.2 Nature of Graphite

Graphite is obtained from naturalmaterials as graphite nodules (Hurlbut and Klein, 1971), and also produced artificially (Olson, 2009), hence is classified into two main categories; natural and synthetic (Ceram Research, 2006). Natural graphite consists of graphite carbon and various degrees of crystallinity and due to its unique properties; it is mined for commercial properties. According to Wikipedia (2008), it contains about 30% of 'beta' form of graphite (which is characterized by hexagonal structure) and can be flat or bracket. Natural graphite is further subdivided into three (3) categories, namely; crystalline flake, amorphous and lump or vein. Crystalline flake graphite usually occurs as isolated flat plate-like particles possessing hexagonal structural edges (Wikipedia, 2008; Microsoft Encarta, 2010). It is found as separate flakes which crystallized in metamorphic rocks in many countries such as Brazil, Canada, China, Germany, Guyana, Japan, Madagascar, Mexico, Sri Lanka, United Kingdom, Norway and India (Olson,

2009). It is less common than amorphous but of higher quality (Olson, 2009). Amorphous graphite occurs as thin particles and is usually formed from thermal metamorphism of coal, during the last stage of coalification or meta-anthracite (Wikipedia, 2008, Microsoft Encarta, 2009). It is characterized by assortment of carbon atoms in a non-crystalline irregular and glass state but not held in a crystalline macro structure. It is present as a powder and constitutes the main component of charcoal, lampblack and activated carbon (Microsoft Encarta, 2008). Amorphous graphite is lowest in quality and most abundant, and is the lowest priced in China, Europe, Mexico, USA and India (Olson, 2009). Lump of vein graphite occur in fissures or veins, fractures, intrusive contacts and appear as massive platy intergrowth of fibrous or acicular crystalline aggregate. It is of hydrothermal origin, (Mitchell, 1993; Wikipedia, 2008; Microsoft Encarta, 2009; Olson, 2009). Vein graphite is the rarest, most valuable and highest quality type of natural graphite and is mined in Sri Lanka (Olson, 2009). Summary of characteristics of the different forms of natural graphite are given in Table 3.

Graphite is also obtained from factory wastes or from Kish produced during iron production process in the blast furnace and from steel making (Waste Management Resources, 1995). Waste streams from the Kish are usually rich in graphite concentrate with high carbon content which needs to be re-cycled to remove valuable materials. Multigravity separation (MGS) and shaking tables are usually used in the graphite recycling process, though some other processes require only screening operations to obtain the valuable materials from the graphite wastes (Waste Management Resources, 1995).

**TABLE 3 SUMMARY OF CHARACTERISTICS OF THE DIFFERENT FORMS OF GRAPHITE**

| FORMS OF GRAPHITE | | | |
|---|---|---|---|
| | **Flake** | **Vein** | **Amorphous** |
| **Description** | Crystalline flakes; coarse >150µm; fine <150µm | Coarse crystals mostly > 4cm | Microcrystalline <70µm |
| **Origin** | Syngenetic; regional metamorphism | Epigenetic; regional metamorphism | Syngenetic; contact and /or regional metamorphism |
| **Ore** | 5 – 30% graphite; stratabound, tabular or lenses | 98% + graphite; veins and fractures | Seams, often folded and failed |
| **Product grade** | 75 – 97% graphite | 98 – 99.9% graphite | 60 – 90% graphite |
| **Main use** | Refractories, brake lining, lubricants and batteries | Carbon brushes, brake lining, lubricants and batteries | Refractories, steel industry, paint and batteries |
| **Major producers** | China, Brazil, india, Madagascar, Germany, Norway, Canada and Zimbabwe | Sri Lanka | China, South Korea, Czechoslovakia, Austria and North Korea |

Adapted from Mitchell (1993)

Synthetic graphite is produced from petroleum coke and tar pitch. It is of high purity, but lower than that of natural graphite (Ceram Research, 2006). It is of two types; electrographite, which is more or less carbon obtained from calcined petroleum coke and tar pitch in electric furnace, while the second type is obtained by heating calcined petroleum pitch to 2800 Kelvin (Ceram Research, 2006). The second type has lower density, higher electric resistance and higher porosity which make it unsuitable for refractors applications. According to Ceram Research (2006), though it contains graphitic carbon as its major compound, it is produced by graphitization or heat treatment of non-graphitic carbon or by chemical vapour deposition from hydrocarbons at temperatures above 2100 Kelvin.

Other useful graphite products include graphene and fullerenes. Graphene sheets are produced when graphite is abraided or exfoliated mechanically when graphite is peeled or can be deposited epitaxially using single crystal silicon carbide or by electrostatic deposition in the form of free-standing film (Wikipedia, 2008; Luque *et al*, 1998). Graphene has some of its properties similar to those of graphite (high thermal and electrical conductivities, lubricity; low noise, large surface area, atomic thickness and molecularly metastable structure), and therefore has potential applications in industries such as construction of quantum computers using anionic circuits, detection of absorbed molecules as in single gas detection, semi-conductors in graphene nanofibers, in construction of ballistic transistors, high carrier mobility in the use of integrated circuits as in an FET channel, electro chromic devices, transparent conducting electrodes as in touch screen, liquid crystal displays, organic photovoltanic cells, and high-emitting diodes; manufacture of solar cells, ultra capacitors, biodevices, [effective against Euclid bacteria (as an antibiotic)], reference material for characterizing electro-conductive and transparent materials and graphene-based thermal interfacial materials (Wikipedia, 2008). Fullerene, ($C_6O$), is an

exotic allotrope of carbon and is obtained by heating graphite to a high temperature. Also called "Buckminster fullerene", its molecules are shaped like tiny soccer balls or bucky balls. Fullerenes are found in ancient rocks in New Zealand and in meteorite-created Rick crater in Germany (Wikipedia, 2008). Fullerene can conduct electricity with no resistance and so can be used as super conductors. Some fullerene tubes are stronger than metals and they could be potential sources of electrical wires or fibers to reinforce plastics to produce composite materials (Wikipedia, 2008). Some other compounds which behave like fullerene and with some $C_6O$ structure seem to inhibit activities of HIV (Wikipedia, 2008).

### 2.1.3 Industrial Characteristics of Graphite

Graphite has unique characteristics. The strength increases with increasing temperature; it is exceptionally good corrosion resistant and immune to thermal shock damage; and its dimensional and thermal stability remain constant at temperature up to 260°C. Due to its excellent corrosion resistance, it is non-fatiguing and so has no property changes with age or cyclic operations (Pyrotek, 2008). It is highly dia-magnetic because it can float in mid-air above a strong magnet (Wikipedia, 2008).

Graphite is also unique because it has the properties of both metal and non-metal (Wikipedia, 2008; Microsoft Encarta, 2009; Olson, 2009). Metallic properties are high electrical and thermal conductivity while the non-metallic properties are high thermal resistance, inertness and lubricity (Olson, 2009). Table 4 (A and B) show the important industrial properties of graphite. Due these unique properties and characteristics, graphite has wide range of industrial

## TABLE 4 (A) INDUSTRIAL PROPERTIES OF GRAPHITE

| **Property** | | **Reference** |
|---|---|---|
| **Formula** | C | |
| **Unit Cell** | a = 2.4612 Ang<br>c = 6.7079 Ang | |
| **Crystal Class** | 6/m 2/m 2/m | |
| **Space Group** | P6_3/mmc | |
| **Formula Units per Unit Cell** | 4 | |
| **Bonding** | Trigonal planar (sp^2)<br>with –C –C – 1.412 Ang | |
| **JCPDS** | 25-284 for 2H (26 – 1079 for 3R) | |
| | | |
| **CONDUCTIVITY** | | |
| **Electrical Resistivity (ohm.m)**<br>**perperndicular to c-axis parallel to c-axis natural** | 9.8 x 10^-6<br>4.1 x 10^-5<br>1.2 x 10^-6 | (Powell & Childs, 1972) |
| **Thermal (Watts/meter.kelvin at 273K), perpendicular to c-axis, parallel to c-axis natural** | 250<br>80<br>160 | (Powell & Childs, 1972) |
| | | |
| **THERMAL** | | |
| **Linear Thermal Expansion Coeff Alpha in units 10^-6K^-1** | 7.8 (at 293K); 8.9 (at 500K)<br>-1.2 (at 293K); -0.7 (at 500K)<br>25.9 (at 293K); 28.2 (at 500K) | (Kirby *et al.*,1972) |
| | | |
| **OPTICAL** | | |
| **Bireflectance and reflection pleochroism** | o-vibration: higher reflectance and yellow or brownish tint<br>e-vibration: bluish-grey tint | (Peckette, 1992) |
| | | |
| **MECHNICAL** | | |
| **Bulk Modulus (Single xtl)** | 34 GPa | Kelly, 1981 |
| **Bulk Modulus (polycrystal)** | 7.3 – 10.7 GPa (non-irradiated uncoated)<br>2.5 – 7.3 GPa (non-irradiated, coated)<br>14.0-16.9 GPa (irradiated, uncoated)<br>7.8 – 8.4 GPa (irradiated, coated) | Boey & Bacon (1986) |
| **Mohs Hardness** | 1 – 2 | |
| **Specific gravity** | 2.2 | |
| **Magnetic** | | |
| **Magnetic Susceptibility**<br>**(Pyrolitic)**<br>**(Pyrolitic)**<br>**(rod)** | Strong diamagnetite<br>-450 x 10^-6 perpendicular to c-axis<br>-85 x 10^-6 parallel to c-axis<br>-160 x 10^-6 | Simon & Geim (2000) |

Adapted from: http://en.wikipedia.org/wiki/Graphite (2008)

## TABLE 4 (B) KEY PROPERTIES OF COMMERCIAL GRAPHITE

| **Property** | **Commercial graphite** |
|---|---|
| Bulk Density ($g/cm^3$) | 1.3 – 1.95 |
| Porosity | 0.7 – 5.3 |
| Modulus of Elasticity (GPa) | 8 – 15 |
| Compressive strength (MPa) | 20 – 200 |
| Flexural strength (MPa) | 6.9 – 100 |
| Coefficient of Thermal Expansion ($x10^{-6}$ °C) | 1.2 – 8.2 |
| Thermal conductivity (W/m.K) | 25 – 470 |
| Specific heat capacity (J/kg.K) | 710 – 830 |
| Electrical resistivity (Ωm) | $5x10^{-6}$ – $30x10^{-6}$ |

After Ceram Research, 2006

applications such as in the mechanical, electrical, electro-chemical, aerospace/nuclear industries, wind and solar industries, medical and chemical process technology, ferrous and powder metallurgy and refractory manufacturing (Wikipedia, 2008; Ceramisis Graphite, 2010). Due to graphite's softness, colour, feel and smudging property, it is used in the manufacture of "lead" pencils (which does not contain lead, but mixture of graphite powder with clay) (Wikipedia, 2008).

Due to inherent softness and lubricity graphite powder is used as a lubricant either by itself or mixed with grease, oil or water (Wikipedia, 2008). Due to graphite's low absorption of X-rays and neutrons, it is used in nuclear industries as a moderator in nuclear reactors where it slows down neutrons without capturing them (Nwobi *et al,* 2002; Wikipedia, 2008; Microsoft Encarta, 2009; Ceramisis Graphite, 2010). Due to its high electrical conductivity, it is extensively used in electrical industries as in the manufacture of carbon brushes, electrodes iron from the blast furnace, generator brushes, electric brushes conductive coating, alkali/manganese long-life-batteries resistors, heaters, susceptors, seed rod, power connectors and sliding contacts.

Due to graphite's high thermal conductivity (melting point = 3650°C) and chemical inertness, graphite is a good refractory material and can be used in the production of refractory bricks, crucibles, moulds, graphite plate, rail road wheel casting (Mitchell, 1993, Wikipedia, 2008; Microsoft Encarta, 2009; Ceramisis Graphite, 2010). Because of its high thermal conductivity, diamond makers can transform graphite into diamond by applying extremely high temperature of between 3000 - 5000°C and high pressure of 100, 000 times atmospheric pressure at sea level (Microsoft Encarta, 2009). High temperature can break strong bonds in graphite so that the atoms can rearrange themselves into diamond lattice. Almost 90% of all industrial diamonds used in the United States are produced in this manner (Microsoft Encarta, 2009).

Graphite can also be combined with other substances such as metal powder, coal, petroleum coke, pitch coke, carbon black and reinforced with fiber and materials with new characteristic properties superior to any of the individual materials alone after undergoing graphitization such as higher thermal conductivities and strength oxidation resistance (Schunk, 2004; Superior Graphite, 2006). While most of these new products have been patented and are being used in industries worldwide, others are in the tertiary steps but with potential applications. Materials from such graphitization can be used to produce synthetic carbon and graphite, graphite fibers, carbon nanofibers, graphite nanofibers, graphite foams, faster run computers, graphite cast, graphite-grafoil tapes, electrographites, nickel graphites, graphite felts, flexible graphite, mesophose pitch-based graphite foams, pitch based carbon/graphite foam, boronised graphite, boronised nitride graphite, polycrystalline graphite (Miroshnikov and Denisenko, 1964; Park et al, 1997; Walker and Booker, 2001; Schunk, 2004; Klett and Kaufman, 2005; Klett and Leicht, 2005(b); Performance Composites, 2010).

### 2.1.4 Exploitation of Graphite

Graphite is mined worldwide using underground and open-cast mining methods. Amorphous and flake types can be mined by the two methods but lump or vein graphite is mined by underground method (Wikipedia, 2008). In the developed countries mining operations are motorized, while in the third world manual labour is used with the aid of simple and cheap implements like buckets and shovels and small pick-up vans for transportation (Wikipedia, 2008). Beneficiation is carried out after mining operations to separate the ore from the waste. Amorphous and vein types do not require serious beneficiation methods; only hand screening is

done before troth flotation. Flake graphite undergoes repeated flotation as the system and lubricity provide 'coating' problems with the gangue or waste particles. During milling, the graphite beneficiation concentrates are sized through screening process and grouped according to size before bagging and usage (Wikipedia, 2008)

### 2.1.5 Limitations of graphite

Despite graphite's wide range of industrial utilization; its use is limited by its tendency to facilitate pitting corrosion into certain categories of stainless steel and to promote galvanic corrosion between different metals due to its electrical conductivity Graphite is corrosive to aluminum in the presence of moisture and that is why some countries like the USA banned the use of graphite lubricants in aluminum aircrafts and aluminum-containing automatic weapons because smallest pencil mark on aluminum facilitate corrosion (Wikipedia, 2008).

Effluents from graphite mills consist of fine particulates which cause health problems to workers, while powdered spillages from the mills also lead to heavy metal contaminations of the surrounding soils (Wikipedia, 2008). Nuclear irradiation generates deformation and stresses within graphite bricks, which results in failures in graphite brick structures especially in the nuclear industries. The irradiation lead to structural changes such as fast neuron damage, radiolytic oxidation (leading to reduction in properties), irradiation creep, irradiation damage to polycrystalline graphite and dimensional changes in hydrocarbon such as coefficient of thermal expansion, thermal resistivity and Young's Modulus (Marsden, 2010).

Simandi and Kenan (1997) pointed out that graphite has certain economic limitations as the price of commercial concentrations of the product is determined by its flake size, degree of

crystallinity, graphitic carbon content, ash content and type of impurities, depending on the applications. Therefore metallurgical and consumer tests are therefore required to market the graphite.

## 2.2 REVIEW OF RELEVANT LITERATURE

On the basis of mineralogical characteristics and mechanism of formation Luque et al (1998) assert that there are two broad categories of natural graphite, namely; a) metamorphic graphite and b) fluid-deposited graphite; (Table 5).

a. Graphite formed due to contact or regional metamorphism of rocks from the conversion of organic matter: from diagenetic process to the uppermost metamorphic grades, the organic matter is channeled naturally through intermediate form before attaining full maturity by graphitization, a process wholly governed by temperature, pressure and chemistry of host rocks.

**b.** Graphite formed from precipitation of solid carbon bearing fluids such as those containing carbon dioxide ($CO_2$) carbon monoxide and methane gas $CH_4$. The fluid-deposited graphite are classified into seven (7) types, namely vein type, which occur as disseminated flakes [such as those occurring in Beni Bousera (Morocco), British Columbia, South Central New Hamsphire (USA), Jurassic alkali basalts (Spain) and Bushveld Complex (South Africa)]; replacement deposits [such as those in fluid-rock interaction in Borrowadale; silicate matter; dissemination as in Serrania de Ronda (Spain), Bushveld, (South Africa); stingers and patches in mafic, ultra mafic mantle xenoliths, coatings and films occurring in vesicles,

**TABLE 5: DIFFERENCES BETWEEN METAMORPHIC AND FLUID DEPOSITED GRAPHITE**

| Characteristics | Metamorphic graphite | Fluid-deposited graphite |
|---|---|---|
| Crystalline size versus grain size | Macroscopic grain size increases as crystalline (unit of crystallographic continuity size increases) | Macroscopically fine-grained (described as "amorphous lumps" commercially) graphite can show maximum degree of crystallinity. |
| Homogeneity of crystallites revealed by HRTEM | Even in high-grade metamorphic rocks, some graphite grains are poorly ordered. | Fluid-deposited graphite is homogenous at grain-to-grain scale. |
| Range in crystallinity | Carbonaceous matter ranges from poorly ordered kerogens to graphite with maximum crystallinity. | With only a few recorded exceptions (a hydrothermal system; in fluid inclusions), natural fluid-deposited graphite concentrations are of very high crystallinity. Examples throughout this paper |
| Temperature versus crystallinity | Linear correlation between DTA temperature maximum and XRD d (002). | Several fluid-deposited graphites lie to the high-crystallinity side of this linear correlation. |

After Luque et al, (1998)

microcracks of submarine basaltic rocks; deposits in fluid inclusions and overgrowth on metamorphic graphite.

Luque et al (1998) observe that the characteristic properties of fluid deposited graphite include marked homogeneity of crystallinity and greater isotropic zoning: Temperature-crystallinity relations of fluid-deposited graphite are more complex than those of metamorphic graphites and they are highly anisotropic, i.e. they have high maximum reflectance values Fig. 6 shows influence of temperature and pressure on the C-O-H system of fluid deposited graphite. According to the workers carbon used for the formation of fluid-deposited graphite are sourced from carbon-bearing compounds released during metamorphism of organic matter, from carbon-bearing compounds released during devolatilization of carbon-rich materials, from igneous rock in mantle and from the host rocks.

### 2.2.1 Occurrences of Graphite

Graphite is known to occur in several places globally. Details of World-wide occurrences of fluid deposited graphite are given in Appendix 1. Simandi and Kenan (1997) reported on the occurrences of cryptalline flake graphite in British Columbia, Canada, noting that the types mainly include disseminated crystalline flake graphite deposits and crystalline flake powder. The workers further described the tectonic setting, depositional environment and age of mineralization, host and associated mineralogy, weathering, genetic models, associated deposit types and ore controls and exploration guides as well as economic factors and limitations of the graphite deposits.

Fig 6

Similarly, Gautneb and Tveten (2008) described the geological setting, exploration and characterization of graphite deposits in Jennestad, Norway. According to these workers, the syngenetic flake graphite deposits in the area are associated with marbles, amphibolites and pyroxene gneisses intruded with different charnockitic rocks and granitic schists which contain up to 40% carbon and distributed as lenses situated 'en echelon' following the main fold structures in the area. Their study reveal that over 30 different graphite-bearing bodies occur in the area, and that about 250, 000 metric tons of graphite with average grade of 20% carbon has been exploited.

Occurrences and utilization of natural graphite in Nigeria has been documented by the Geological Survey of Nigeria Agency and some workers. Dada (1981) reported on the occurrences of schistose graphite interbedded with gneisses in Dutsen Hai, Kano State. Documentation by the Geological Survey of Nigeria (1987) revealed the occurrences of graphite at Mayo Butale in Adamawa State; Hosere Nuwa, Gayan and Jauro Jalo in Taraba State; Birnin Gwari in Kaduna State; Haya and Ningi in Bauchi State, Dutsenma in Kano State and some traces in South – East and South – West Nigeria. Also Adegoke *et al*, (1989) reported graphite occurrences at Dutsen Ma in Katsina State.

Nwanebi (2000) indicated that graphite occurs at Alama in Niger State, Birnin Gwari (Kaduna State) and Dutsen Hai in Bauchi; and Garba (2002) reported the occurrences of graphite associated with sericitic phyllites at Tsohon Birnin Gwani in the Kushaka schist Belt of North – Western Nigeria. These dark grey graphite phyllites act as host rocks to gold, sulphide minerals (iron sulphides such as pyrite 60% and marcasite 40%) with minor sphalerite chalcopyrite, pyrrhotite, galena and magnetite. Ekwueme (2003), reported of graphite occurrences with gneisses in Obudu area, positing that the graphite was formed during granulite facies

metamorphism in Obudu Plateau, South-Eastern Nigeria, and that it was the main source of carbon dioxide ($CO_2$), the major component of the fluid phase, for the metamorphic activities.

Nwobi *et al* (2002) carried out the beneficiation and characterization of graphite occurrences at Dutsen Haiyar, Bauchi State. Parameters determined include flake size, density, ash and carbon content and the result obtained showed Bauchi graphite is of high quality.

### 2.2.2 Industrial Application of Graphite

Graphite can be applied in the refractory, electronics, electrical, chemical, aerospace/nuclear/power, mechanical and metallurgical industries on the basis of its properties, origin and types. After several studies on graphite, Hurlbut and Klein (1971), submits that industrial utilization of graphite is best assessed based on its physical properties, composition and structure (including the determination of colour, feel, streak, fusibility, specific gravity, attack by acid, cleavage, hardness, luster, colour, feel, streak fusibility, specific gravity, attack by acid, cleavage, hardness, luster, flexibility, elasticity and tenacity. Likewise, Lakin (1997) discussed rising demands of graphite products, especially graphite electrodes in highly industrialized economics on the basis of graphite properties such as thermal shock resistance, mechanical strength, electrical resistivity and ultrasonic transmission velocity. Mitchell, (1993) did extensive research work on geological occurrences, properties and beneficiation of graphite, upon which the worker characterized the different forms of graphite and classified beneficiated graphite (Table 6) for different industrial applications. Also, Wikipedia (2008) discussed the properties and industrial applications of carbon and graphite felts based on their unique

**TABLE 6: SPECIFICATIONS OF BENEFICIATED GRAPHITE FOR DIFFERENT APPLICATIONS**

| Application | Type | C Content | Flake size | Comments |
|---|---|---|---|---|
| Refractories | | | | |
| Magnesia graphite | F | 85 – 90% | 150-170 µm | Ash<2%, often up to 10% |
| Alumina graphite | F | Min 85% | 150-500 µm | |
| Crucibles | AF | 80-90% | +150 µm | Bulk density 48-54g per 100cm$^3$ |
| Exapnded graphite | F | Min 90% | 200-1700 µm | |
| Foundry additive | AFV | 40-70% | 53-75 µm | Sulphides and other readily fusible minerals undesirable |
| Foundry core and mould washes | AF | 70-90% | ~75 µm | |
| Brake/clutch linings | AFV | Min 98% | <75 µm | |
| Bearings | FV | 90-93% | +150 µm | |
| Lubricants | AFV | 98-99% | 53-106 µm | Free from sulphides, abrasive material and metallic contaminants |
| Dry cell batteries | A | Min 88% | 85%<75 µm | No metallic impurities such S less than 0.5% |
| Alkaline batteries | AF | Min 98% | 5-75 µm | No impurities such as Cu, Co, Sb and As |
| Recarburizing steel | A | 98-99% | ~5 µm | |
| Carbon brushes | AFV | 95 – 99% | <53 µm | <1% ash/silica. No abrasive or metallic contaminats |
| Electricals | FV | 93 – 95% | +150µm | |
| Pencils | AF | 95 – 97% | +150 µm | Free of gritty impurities |
| Conductive coatings | A | 50 – 55% | <75 µm | May contain up to 25% silica, but free from gritty impurities |
| Packing paints | FV | 85 – 90% | <150 µm | |
| Polishes | AFV | 85 – 90% | <150 µm | |
| Drilling and lubricating | F | 80% | N/A | About 4\|b per n=barrel of mud |
| Explosives (control of burning rate) | AF | 65% | <150 µm | Free from sulphide and acids. Low moisture content |
| Nuclear reactors (Moderators and reflectors) | F | 93 – 95% | N/A | Free from high neutron absorbing elements, e.g. boron |
| Boilers (scale prevention) | F | 50% | N/A | |

Key:
A = Amorphous
F = Flake
V = Vein
N/A = Not availabe

Modified from Miichell, 1993

properties including low thermal conductivity and specific heat, high thermal stability, shape retentivity, low absorption of gases or vapour, erosion resistance and low ash content for the graphite felts. Pyrotek (2008), fabricator of graphite and graphite products, agrees that the

graphite's unique properties such as immunity to thermal shock resistance, constant dimensional stability, good corrosion resistance, non-fatiguing and lack of changes in properties with age or cyclic operation which aid in the production of various graphite components that include fluxing tubes, flow control systems, degassing components and specialized applications such as aerospace, electronics and unclear products. In addition, Performance composites (2010) highlights that the industrial utilization of graphite composite materials is based on their high specific stiffness, strength and low coefficient of thermal expansion.

As research and industrial improvement of graphite and graphite materials increased through the decades, Kindler (1983) carried out studies on oxidation-reduction of carbon and graphite materials in order to improve their grades by impregnation them with phosphorus compounds treatment from 350°C - 800°C. The study showed that the oxidation resistance of industrial carbon and graphite grades could be improved by impregnation with phosphorus compounds of certain metals.

Revilock (1990) of Union Carbide Corporation, USA described "Grafoil", as a new form of graphite product which has no bonding agents, resins or rubber compounds which is manufactured by a process where graphite particles are rolled into sheets between 5 – 10mm thick. The product has high degree of flexibility, tensile strength, compressibility and low permeability whose industrial uses include production of gaskets for flange joints and pickings for seals. Bacos (1993), posits that on the basis of the good mechanical performance of carbon

and graphite materials in industrial structural carbon and graphite composites have been identified for potential uses in future-manned hypersonic vehicles and other aircraft applications. Mechanical applications of graphite and graphite products/composites are shown in Appendix 5 (a and b).

Park *et al* (1997) experimented on the storage of hydrogen gas in graphite; nanofibers produced by decomposition of ethylene, carbon monoxide and hydrogen or selected metal powders at high temperatures of 600°C and discovered that when exposed to hydrogen at 2000 psi pressure, graphite nanofibers can absorb and store up to 40 percent lot % of the hydrogen gas. Similarly, Baker (1998) while investigating the use of graphite nanofibers for hydrogen storage industries observed that metal catelysed decomposition of hydrogen carbon occur during synthesis of graphite material at 400°C - 800°C to form nanostructures consisting entirely of graphite platelets and some amount of amorphous carbon. Lueking et al (2005) posits that during decomposition, the graphite lattice in the nanofibers is expanded through carbon exfoliation and thermal shock resistance to open up the interplanar spacing between the graphite layers, thus creating defects and dislocations within the nanofibers, hence its storage capability.

Coursey *et al* (2005) discussed experimental performance and use of mesophase-pitch-derived graphite foam as an evaporator for cooling electronics, highlighting its principal properties that may produce excellent result such as its low density, high thermal diffusivity, high open porosity, thermal conductivity and low coefficient of thermal expansion close to that of silicon. Klett and Kaufman (2005) report that water from water chamber in graphite foam is used as a heat transfer medium in an air-based cooling system, while Klett and Leicht (2005a) report that evaporators made of high thermal conductivity graphite foam is used in cooling electronic chips which spreads heat at 150w/$m^2$ at chips temperature of 71°C. This observation

represents more than 400% improvement in cooling power compared to the current metal aluminum or copper oxide microprocessors.

These researchers therefore affirm that it is possible to generate nanofibers with graphite platelets, based on the crystallographic orientation of the faces existing at the metal-carbon interface as given in Fig. 7 (a and b). This work is of futuristic importance as it confirms possible conversion of chemical energy to electrical energy to drive electric vehicles with hydrogen stored in nanofibers; hence would aid the on-going research aimed at producing ideal fuel and more efficient engines to replace the current combustion engines whose efficiency is being threatened by pollutants.

Flexible Graphite materials are extensively used in electronic industries for electromagnetic interference (EMI), gasketing, resistive heating, thermoelectric energy generation and heat dissipation. These applications are based on graphite's unique properties such as flexibility and compliance especially as interface materials (electromagnetic thermoelectric, or thermal), resilience, impregnation and chemical and thermal resistances. Klett (2002) and Klett *et al,* (1998) and Klette (2002) carried out series of experiments and tests on the development of carbon and graphite based products including mesophose derived, pitch-based carbon form and composites, materials for new space technologies, faster run computers, ultra-efficient light-weight radiators, microclimate and evaporative cooling and efficient heat sinks (Fig. 8). The workers found out that due to the continuous reinforcement and interconnected network of a graphite ligaments the team materials and products exhibit higher isotropic thermal conductivities and better mechanical properties such as unique shear strength, toughness, dimensional stability with low coefficient of thermal expansion and modulus, high apparent bulk density and creep resistance than ordinary carbon fiber reinforced materials. Lu and Chung

Fig 7 (a and b)

Fig 8

(2002) discussed the oxidation of carbon and graphite materials at high temperatures, as it affects such products as poly-crystalline graphite and pitch-based carbon timber material which vapourises at temperatures above 812°C. The workers found out that the polycrystalline graphite can be protected from acid attack using phosphate solution (especially by treating the surface of the materials with phosphorus acid, ($H_3PO_4$). In the same vein, Walker and Booker (2001) discussed the results of an invention that seeks to protect carbon/carbon composites and graphite materials at elevated temperatures above 850°C especially, in carbon/carbon aircraft brake system. Phosphoric acid based penetrate salt solution was used in the series of experiments to inhibit oxidation of the carbon/carbon and graphite materials at high temperatures. The workers found out that open porosities (5-10%) of conventional carbon/carbon composites was the principal cause of internal oxidation of carbon/carbon composite material installed in around the brake rotor lugs of airplanes and that protection of these composites could be achieved by acid-phosphate impregnation.

Investigations by Pihura and Oruc (2007) indicates that spheroidal graphite iron (SGI) could be applied as a substitute for steel casting in view of its properties such as better castability, easier mechanical moulding, lower friction, lower investment cost and energy consumption, melting temperatures, higher field and less expensive than steel castings.

The development of graphite's new product, "graphene hybrid material" was discussed by Lee and Lee (2009), who patented the production of this material using chemical vapour deposition (CVD) method, i.e. when graphene bonded with a matrix ("epitaxically grown"). Graphene is one atom-thick planar sheet of $sp^2$-bonded carbon atom that is densely packed in a honey-comb crystal lattice, and is known to be the strongest material in the world (Wikipedia, 2008). Crystalline flake graphite consist of many graphene sheets, stacked together with

interplanar spacing of 0.335nano meter (which means a stack of 3 million sheets of grapheme would only form one millimeter sheet of graphite thick).

Despite their unique properties and wide range of industrial applications of graphite products, Marsden (2010) however reported of major stresses and deformations in graphite bricks in industries, and attributed them to changes due to irradiation, radiolytic oxidation, weight loss, dimensional changes in oxidizing environment, and thermal and creep strain, among others. Several attempts are made to redress observed deficiencies in properties of graphite. Miroshinkov and Denisenko (1964) assessed the operation of nickel-graphite compositions in steam atmospheres at high temperatures and pressures with a view to develop new industrial materials which could operate in corrosive environment efficiently. Natural graphite is known to have low solubility in nickel at high temperature; hence thermodynamic calculations were employed to evaluate the performance of the nickel-graphite materials at high temperature (55°C) and pressure (90 atm). Boylan (1996) while studying carbon-carbon composites and carbon-graphite pointed out that artificial graphite material has unique properties which are upgraded to improve on industrial properties of natural graphite. These include increase in modulus of elasticity, thermal conductivity and thermal shock resistance, strength, heat resistance in non-oxidant atmospheres, abrasion resistance, electrical conductivity and low coefficient of thermal expansion, density and coefficient of friction and non brittle failure.

Tatas (2008) carried out beneficiation and characterization of Adamawa graphite, Toungo by froth foliation method to improve its purity for possible industrial utilization. Results of beneficiation showed that Walon Kole flake graphite can be upgraded from 39.6% carbon to 85% while Mayo Butale graphite can also be upgraded from 33.3% to 73.4%. Their values fall within good grades for industrial utilization.

# CHAPTER THREE

# METHODOLOGY

The study is divided into three (3) unit operation, namely; field study, detail laboratory analysis and synthesis of the analytical data.

## 3.1 FIELD STUDIES

These are divided into five (5) parts as follows:-

a) Preliminary appraisal of information documented in the Reconnaissance Geological and Mineral Resources Survey (2004) report, Adamawa State. The aim was to have first-hand knowledge of the area in terms of landscape, general geology, accessibility and mineral occurrences.

b) Identification of physiographical characteristics of the project area from topographic maps and traversing.

c) Identification of rock samples in the area and their lithological contacts on the scale of 1:26, 000.

d) Sampling of all encountered graphite exposures and associated rocks in the area.

e) Field treatment of sample; washing, crushing or grinding the samples into smaller pieces. This was carried out to avoid contamination and to put them into transportable form.

### 3.1.1 Geological Mapping

Systematic geological mapping was carried out in the area between December, 2007 and July, 2008. the field equipment and materials used include the following; Thuraya Global Positioning System (GPS Model ASCON Hughes), Compass Clinometer (Silver), geological hammers (Nos 0.75kg with wooden handle and 0.05kg with metallic handled), hand less (X12), two nos. 1;50,000 contoured topographic map sheets; Dau 257 NE and Kiri 237 SE by Federal Surveys, 1969, 1971, enlarged to 1: 26,000, log books (with hard covers), digital and still camera, small hand bag for carrying rock samples, binocular microscope, masking tape, hand-held magnets, field shoes. Metric rulers (30cm plastic and 1m wooden T-square), pencils, (1H and 2B) coloured pencils, erasers (Tikky 20, protractor, based board (50cm x 50cm ply wood), tape measure (5m), regional 1:250, 000 geological and fracture analysis map, food supplies, water and hat. Other materials were safety goggles, selotapes (masking and transparent), 2 chisels, two 1:250, 000 based maps by Consulint (1976), 3 razor blades, 3 sharpeners, two reference materials, "Field Mapping for Geology Students by Ahmed and Almond (1983) and "Thesis and Technical Reports in Geology and related Sciences" by Ogezi, (1996), some medications in a mini first aid box and 2 pen knives and a field vehicle. There were four field assistants and guides and three vigilante security personnel from Toungo Local Government Area as the location share boundaries with Gumti National Park where there are wild animals.

Equipped with all required field materials, a temporary base station was chosen. Due to the size of the project area (28.4km$^2$), the area was divided into three hydrological units for ease of mapping (Fig 9a). The units were mapped sequentially from area 1 (North of Federal Trunk 'A' road up to 8$^o$ 00' 00" N) then area 2 (from 8$^o$ 00' 00" to 8$^o$ 01' 00" N), and area 3 (South of

Fig 9a

Fig 9b geologic map of the project area

Fig 9c structural map of the project area

the Federal Trunk 'A' road to the borders of the Gumti Game Reserve (Fig. 9b and c) the area around Mayo Butale up to the quartzitic dyke, about 2km southwest, however lies within the Game Reserve.

In carrying out this field survey, the following steps were adopted.

1) Locating oneself with reference to a temporary base station by making reference to known physical feature which can clearly be seen on the topographic map.
2) Taking traverse along chosen routes
3) Locating outcrops and again my bearings from the outcrop, noting all superficial covers.
4) Detailed description of the outcrops and other structural features on the outcrop such as strike of plane surface and dip of joints.
5) Collection of samples for detailed field study, for chemical analysis, this section and for metallurgical studies.
6) Macroscopic classification of all samples collected (i.e. hand specimen). Noting every observation in the field book, with sketch as well as on the 1:26,000 topographical map.

Observations at each exposure include location point, locality number, texture (grain size or fabric), colour of the rock and attitude of the structures. Station 1 is an exposure close to a hill and the location was obtained by taking GPS and compass readings of three known physical features that are clearly seen on the topographic map. The first feature is Gudaru Hill, while the second is Hosere Gofire and the third, 'graphite' Hill as shown on the physical sketch below All GPS equipment used in the country are usually standardized with Minna Datum Niger State except for the Thuraya GPS which has already been standardized from the factory.

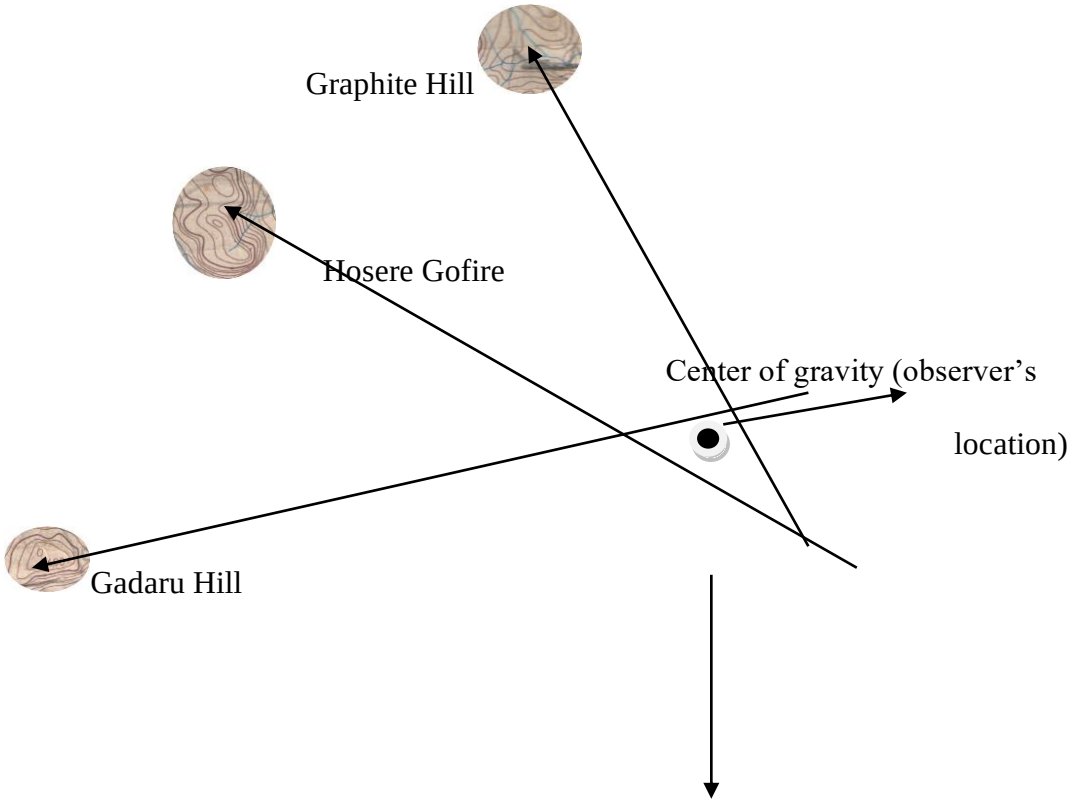


GPS reading: N7° 59' 05.72"

E11° 58' 05.69"

HASL: 673meters

Time: 12:44.022pm

Fig. 10: Measurements during traverse mapping

However, during traversing, 5° 07' was added or subtracted from the compass readings while using Dau sheet 257 NE due to magnetic variation and 5° 18' while using Kiri sheet 237 SE. This is demonstrated in Fig. 11 (A and B). Bearing of the location was obtained with the GPS

Fresh portion of the exposure was broken off with the aid of hammer and chisel. Sample 1A was macroscopically described and recorded in the field note book. Sample 1A is pink-coloured, holocrystalline, medium to coarse-grained rock with visible quartz grain and feldspar phenocrysts, flex of biotite and muscovite, other very tiny opaque minerals. On the basis of the constituent feldspar, quartz and mica minerals, the rock is granitic, probably biotite granite. The rock was formed from slow cooling at depth under high temperatures due to its grain size (Nockolds *et al,* 1979). The fresh sample was broken into three pieces with the stainless head of the smaller hammer; one piece for field treatment meant for chemical analysis, while the other two were for thin section and metallurgical tests. The samples were cleaned with white clean cloth, after which two were bagged and labeled while the third was crushed to -5 to 1cm size with a stainless hammer and dried on a white paper under a shade to remove water and also to avoid contamination. The sample was put into leather a bag which was in turn put into brown envelopes.

The next station (named 1B) is located about 1.5km NNW of station 1A. The process undertaken at station 1 were repeated at the new station, i.e. taking bearing with GPS, breaking off fresh sample and further breaking it into 3 parts, macroscopic description of the sample, cleaning the samples, recording all observations in the field note book and on the typographic map, bagging and labeling two of the three samples for thin sectioning and metallurgical tests.

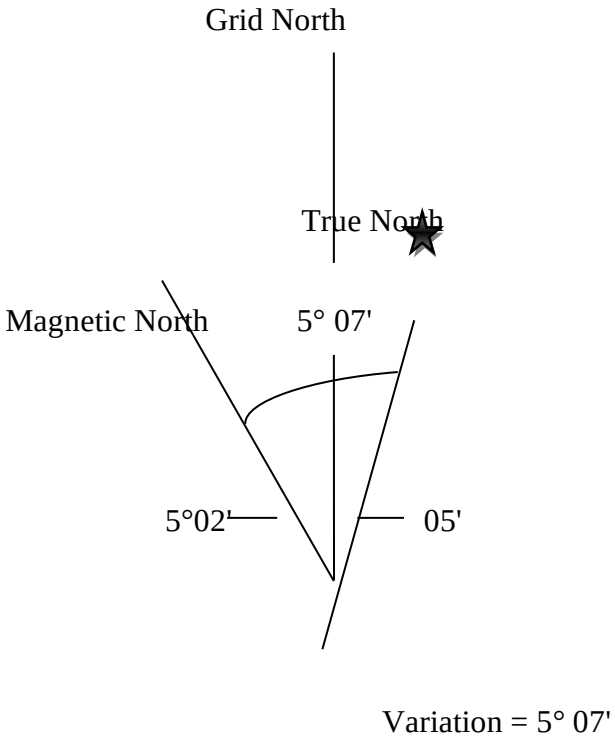


Fig 11 (a) Magnetic Variation, Dau sheet 257 NE, (After D.O.S., Federal Surveys, (1965), Dau Sheet 257 NE, 1:50, 000)

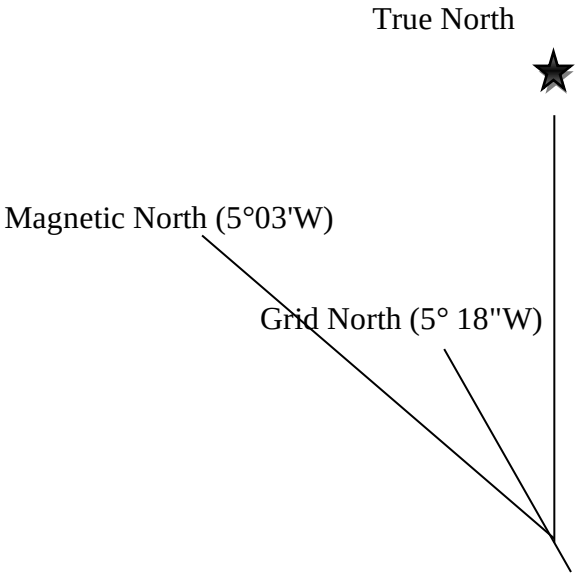


Fig: 11 (b): Magnetic variation, Kiri 237 SE, (After D.O.S, Federal Surveys, Kiri sheet 237 SE, (1965), Kiri sheet from 8°00 north) (Global positioning system) to be N70° 99' 05.72" E11° 58' 05.61").

Measurements and description of structures found on the in-situ exposed host rock were done and recorded in the field book and on topographic map. During the geological mapping exercise attention was paid to marking out the boundaries of rock types 1A and 1B by using the GPS, plotting the coordinates of the rock boundaries on the map and joining them, after the actual mapping work, several field trips were undertaken to the project site to confirm certain rock boundaries especially in the hilly terrain and some structural features as shown in Fig. 9b.

### 3.1.2 Sampling

#### 3.1.2.1 Sampling Method

Lithologeochemical survey method was adopted for this study as best results are obtained from in-situ samples. Traverse system was used for sampling but spacing was irregular due to non-availability of exposures in some of the areas especially the Southern-most of the areas especially the southern-most parts up to the North-East within zone 3 in Fig 10. The whole area was traversed; the three (3) fresh in-situ samples were collected from each of the rocky outcrops. A total of thirty-three (33) samples were collected from eleven sampling points and properly labeled. All the sample points were marked on the topographic map.

The samples were collected in threes (i.e. 3 from each outcrop) in order to obtain adequate samples for the three basic tests; thin section, physical tests and chemical analysis. The samples were taken, cleaned and variedly labelled for the different tests. For thin sectioning, about 300gm bulk/lump of each sample was labelled 1A, 2A, 3A, 4A, 5A, 6A, 7A, 8A, 9A, 10A AND 11A for metallurgical and consumer tests; about 400gm bulk/lump samples were labeled

1B, 2B, 3B, 4B, 5B, 6B, 7B, 8B, 9B, 10B, and 11B and for chemical analysis, about 200gm of lump samples were labeled 1C, 2C, 3C, 4C, 5C, 6C, 7C, 8C, 9C, 10C and 11C.

#### 3.1.2.2 Sample Preparation

Eleven (11) representative samples meant for detail laboratory analysis were crushed with the stainless head of the hammer and sieved using a local sieve mesh of -1 to +3. The coarse sizes were discarded and about 100gm the fines were bagged, labeled transported to the base. At the base the samples meant for chemical analysis were further pulverized and then treated with concentrated nitric acid ($HNO_3$) to decompose in order to breakdown the chemical bond for easy extraction of the constituent elements. Concentrated nitric acid was used because of the attainable high temperatures and oxidizing effect yield of highest elemental proportions.

## 3.2 LABORATORY INVESTIGATIONS

The samples were subjected to laboratory tests including chemical analysis, petrographic studies and physical, metallurgical and consumer tests.

### 3.2.1 Chemical Analysis

Chemical analysis of the rock samples were conducted on ten of the eleven samples at Aston Microscopy and Engineering Laboratory, Aston University, United Kingdom and at the Nigerian Metallurgical Development Center (NMDC), Jos. The rock samples analyzed in the U.K include 1A, IB, IC, ID, 2A, 2C, 7, 8, 9 and those analyzed at NMDC, Jos include 1C, 2A, 2B, 7, 8 and 9. Both graphite samples A and B were analyzed at the two institutions. At both

laboratories, the analyses were undertaken using Energy Dispersive X-Ray Fluorescence Spectrometry (EDXRF). At Aston University laboratory, the XRF equipment has an attached scanning electron microscopes fitted with a digital camera and computer central imaging with a printer. The microscan equipment analyses at high magnification with exceptional depth of field to allow detailed microstructural examination of the samples. The ED-XRF is a non-destructive method of quantitative and qualitative elemental analysis of solid and liquid sample materials. In this process, the high energy content of an x-ray beam causes a sample to generate x-rays characteristics of the atoms in the sample (when inner K, L or M electrons are removed from target atoms and outer electrons fill the vacancies. Elements present in the sample are identified from the energies of this characteristic radiation, and concentrations are evaluated from intensity measurements (Chagga, personal communication).

Twenty grams (20g) of the graphite sample was finely ground to pass through a 200 – 250 mesh sieve, dried in an oven at 105°C for 1 hour and then cooled. Thereafter, the sample was intimately mixed with a binder in the ratio of 5g sample(s) to 1g cellulose flakes binder and pelletized at a pressure of 10-15 tons/inch$^2$ in a pelletizing machine. The pelletized sample(s) were then stored in desiccators for analysis. At the NMDC, Jos, the machine (ED-XRF) was switched on and allowed to warm up for two hours. Appropriate programs for the various elements of interest were then employed to analyze the sample materials(s) for their presence or absence. The result of analysis could be reported either in parts per million (ppm) or percentage (%) for minor and major elements; but percentage was however adopted or this work. At Aston University laboratory, the already prepared samples were fed into scanning electron microscope which is connected to the EDXRF equipment. Points on the sample were scanned with precision and targeted with X-ray beam and then bombarded. The inner electrons of the different elements

in the sample were therefore activated. Fluorescent x-rays of a wavelength characteristic of the activated element were emitted and their compositions were therefore determined quantitatively. Elemental maps of the samples in the scanned points were also produced to identify where individual elements are concentrated within the samples (Appendix 3 A to J, with the intensity of energy of bombardment plotted against the wavelength of the element).

### 3.2.1.1 Oxide Determination

Oxides are chemical compounds that are formed by the reaction of oxygen with other elements, particularly at elevated temperatures. However, the noble gases helium (He), neon (Ne), argon (Ar), krypton (Kr) and xenon (Xe) and noble metals like gold (Au), silver (Ag) and platinum (Pt) do not combine with oxygen. During the chemical and determinative analysis on the rock samples, only the elemental weight percent were determined. The oxide form was later determined by empirical formula.

$$\frac{\text{Atomic mass of the element + Atomic mass of oxygen}}{\text{Atomic mass of the element}} \times \text{weight of the element}$$

For instance, to determine the oxide form of Aluminum, A1

Oxide form = $Al_2O_3$

Atomic weight of Aluminum = 27 x 2 = 54

Atomic weight of oxygen = 16 x 3 = 48

Weight % of Aluminium determined from analysis = 10

The oxide $A1_2O_3$ is given by $\frac{27 \times 2 + 16 \times 3}{54} \times 100$

### 3.2.2 Petrographic Analysis

#### 3.2.2.1 Thin Section Preparation

The thin sections were prepared in the petrological laboratory, University of Jos. The following stages were involved in the preparation of the thin sections.

1. Cutting: the crystalline rocks were cut or trimmed into the shape and size of the glass slide using, the cutting machine. This gave the rock the desired section.
2. Lapping: One surface of the rock section was glued using silicon carbide (abrasive) to make it smooth and parallel (flat).
3. Frosting: One surface of the glass slide was made less smooth by grinding it with silicon carbide (600gm). This was done so as to give a strong bond between the rock section and the glass slide after gumming them together.
4. Mounting: The rock section was glued to the glass slide (on a hot plate) using araldite as the mounting medium.
5. Trimming: The thickness of the rock section was timed significantly using the cutting machine after 24hours of mounting.
6. Grinding; the thickness of the rock section was further reduced in a gradual grinding process using the grinding machine until the rock section was transparent under the transmitted light of a polarizing microscope with the interference color of quartz appearing yellow.
7. Thinning: The rock section was gradually grounded manually on a lapping board using silicon carbide 800grit. This was done until the standard thickness of

0.03mm or 30μm was attained using the white grey interference colour of quartz as index reference.

8. Labelling/Covering: The thin rock section slide was labeled (i.e. sample number was written on the slide), after which the thin rock section was covered with a glass cover using araldite.

#### 3.2.2.2 Mineral Identification

The thin section was studied under a polarizing microscope and the mineral constituents identified. Observation of the various optical properties were done under both plane polarized light (PPL) and cross polarized light.

### 3.2.3 Physical, Metallurgical and Consumer Tests

Simandi and Kenan (1997) and Gautneb and Tveten (2008) discussed that physical, metallurgical and consumer tests are required to market flake graphite as the tests affect its economic factors. The most important of these tests include flake size, degree of crystallinity, graphitic carbon content, ash content and type of impurities. Other important factors include bulk density, porosity, modulus of elasticity, compressive strength, flexural strength, coefficient of thermal expansion, thermal conductivity, heat and specific heat capacity and electrical resistivity.

These tests can be divided into three broad categories, namely; physical tests, proximate analysis test and metallurgical/determinative tests. The physical tests include bulk density, porosity and cold crushing strength; proximate analysis tests include moisture content, volatile

matter, ash content and fixed carbon content and metallurgical tests include modulus of elasticity, compressive strength, thermal conductivity, specific heat capacity, electrical conductivity, thermal shock resistance and flexural strength. These tests were conducted on the graphite samples at the two centers. The bulk density, flake size, porosity, cold crushing strength, thermal shock resistance, ash content, volatile matter and moisture content were conducted at the Coal Department of the Nigerian Metallurgical Development Centre, while other parameters such as thermal conductivity, compressive strength, specific heat capacity and electrical resistivity were carried out at Department of Physics, University of Jos.

#### 3.2.3.1 Physical Tests.

**a. Bulk Density:**

Bulk densities of the graphite samples were determined by volume method using mercury and tecramics densometer (a 1991 model from Fairey Tecramics Ltd, UK). A densometer comprises a physical balance micrometer, a pairy crucible tongs, a 100ml beaker and 2kg-weight of mercury (Fig. 12)

The physical balance was placed on the laboratory bench so that the center of the weighting pan lies under the saddle. A spacer sleeve was provided to prevent the saddle from hitting the base of the beaker when in position on the balance pan. Two regular cylindrical shape specimen of each of the two graphite samples were used for the test. Each of the specimens was

Fig 12: Tecramics Densometer

weighted in the top-pan physical balance (with an error level of $\pm$ 0.01gm) and the weights designated as $W_1$.

Then thousand gram weights (1kg) of clear mercury was poured into a 100ml beaker and placed centrally on the balance pan under the saddle. The saddle was then lowered into the mercury by means of a hand wheel and then locked with the bridge locking screw. The micrometer was adjusted repeatedly until the pointer just touches the surface of the mercury, and the gram scale of the balance reads zero.

The saddle was then raised by means of a hand wheel and the specimen placed on the surface of the mercury using crucible tongs. Afterwards the saddle was then lowered so that the specimen was immersed completely in mercury. The bridge locking screw was then locked and the micrometer adjusted until the pointed just touches the surface of the mercury. The balance was then read (to $\pm$ 0.01gm) and the new weight was recorded as $W_2$. The balance was then raised and the specimen sample removed from the surface of the mercury by means of crucible tongs. Temperature of the mercury was maintained at 24˚C during and after the experiment.

**b. Cold Crushing Strength (CCS)**

Apparatus used for determination of Cold Crushing Strength (CCS) include 2 pieces of graphite samples (A and B), and a small card board of about 63cm in thickness.

A piece of each of the two graphite samples was used for the test. Sample A was 3cm long and 2cm wide (Area = $6cm^2$), while B was a cube of 2.5 x 2.5cm ($6.25cm^3$). A 63cm thick card board sheet was placed between platens of the hydraulic press and the bearing face of the graphite cube. Load was applied and steadily increased until the cubes failed to support to

support the lord. The maximum recorded load was taken as the crushing load which is obtained from the relation.

CCS = M/A

Where M = Mass or load applied, and

A = Area of the piece of graphite

**c. Porosity**

Porosity of a given undisturbed material is the ratio of the volume of pores or open spaces in the solid to the total volume of the undisturbed material and it is expressed as a percentage (Todd and Mays, 2005). Porosity of the graphite samples were determined under observed conditions, hence apparent porosity is used.

The specimen (a 2.5x 2.5cm cut test piece) was dried in an oven at 110°C to a constant weight (D) with accuracy of 0.1gram. The dried specimen was then suspended in distilled water in a 300L beaker such that the specimen does not touch the bottom or sides of the container. The specimen was boiled inside the water for two (2) hours, cooled to room temperature and weighed (as S). The specimen was then removed from water and wiped dry by lightly blotting its surface with a wet towel. It was then weighed in air (W).

The 'apparent porosity' (P) was then calculated by the formula

P = VI/V x 100

Where VI = Actual volume of open pores of the specimen (CC) = W – D)

V = External volume of the specimen = W – S

### 3.2.3.2 Proximate Analysis Tests.

These involve determination of ash content, volatile matter, moisture content and fixed carbon. For these tests, the samples were pulverized, further grounded and sieved through a 0.25mm sieve mesh to obtain a powdery graphite sample.

#### a) Ash Content Determination

This test measures the amount of inorganic mineral residue which cannot burn in the material. Apparatuses used for the tests include crucibles, muffle furnace, desiccators and weighing balance. The crucibles were first heated in the muffle furnace for about 30 minutes to obtain stable weight. About 1gm of the prepared powdered graphite sample was obtained and placed in an open crucible. It was then heated in the muffle furnace for one hour at about 825˚C, after which it was allow to cool in the desiccators and weighed. The percentage ash content of the sample was calculated from the formula:

$$\frac{\text{Weight of residue}}{\text{Weight of sample}} \times 100$$

**b) Determination of Moisture content**

Apparatuses used for this test were the same as for the ash content. One gram of each of the graphite samples were put into two crucibles and closed. They were heated in oven for about one hour at 110°C. The samples were then cooled in the desiccators and reweighed. The moisture content of the two samples was then calculated from the formula.

$$V.M = \frac{\text{Difference in weight after heating}}{\text{Original weight of sample}} \times 100$$

**c.) Determination of Volatile Matter**

Apparatuses used were the same as for ash content. One gram of prepared graphite material was obtained and put into a crucible. Benzene was then added to increase its volatility and the crucible was then covered. It was then heated in the muffle furnace for about seven (7) minutes at 900°C, allowed to cool in the desiccators, and then reweighed.

The volatile matter was calculated from the formula

$$\text{Volatile matter} = \frac{\text{difference in weight after heating}}{\text{Weight of original sample}} \times 100$$

**d) Determination of fixed carbon**

Fixed carbon is the total inorganic material in the sample. It is calculated from the total percentages of ash content, volatile matter and moisture content of the samples.

### 3.2.3.3 Metallurgical Tests

a) Determination of Thermal Conductivity, Heat Capacity, Specific Heat and Electrical Conductivity of Graphite (Bad Conductor) using Lee's disc method.

The following apparatuses were used: Retort stand, thermometers, brass block, condenser and stem chest as shown in Fig, 13.

Apparatus for determination of thermal conductivity using Lee's Disc method. First, the thermometers were rubbed with petroleum jelly to ensure good thermal content. Heat was then passed from the steam chest through the brass blocks to the specimen using two channels where the two thermometers were fitted. The steam was passed gently until a steady temperature was attained for both $T_1$ and $T_2$. The temperature of the blocks rose until heat reaching them was lost to the atmosphere while some were used by the specimen. The heat was then put off and $T_1$ and $T_2$ observed at a minute interval and the specimen was allowed to cool.

The rate of fall of temperature was found by plotting a graph of temperature against time. The specific heat (quantity of heat required by a unit mass of the graphite sample to raise its temperature by 1°C) was also found from the graph.

**b. Compressive Strength**

Compressive strength is the maximum strength at which an undisturbed natural material or rock deforms or fails under an applied load. It depends on the internal forces of the material. The equipment used for the measurements was F-Test Seidner model D7948-Universal Testing Machine.

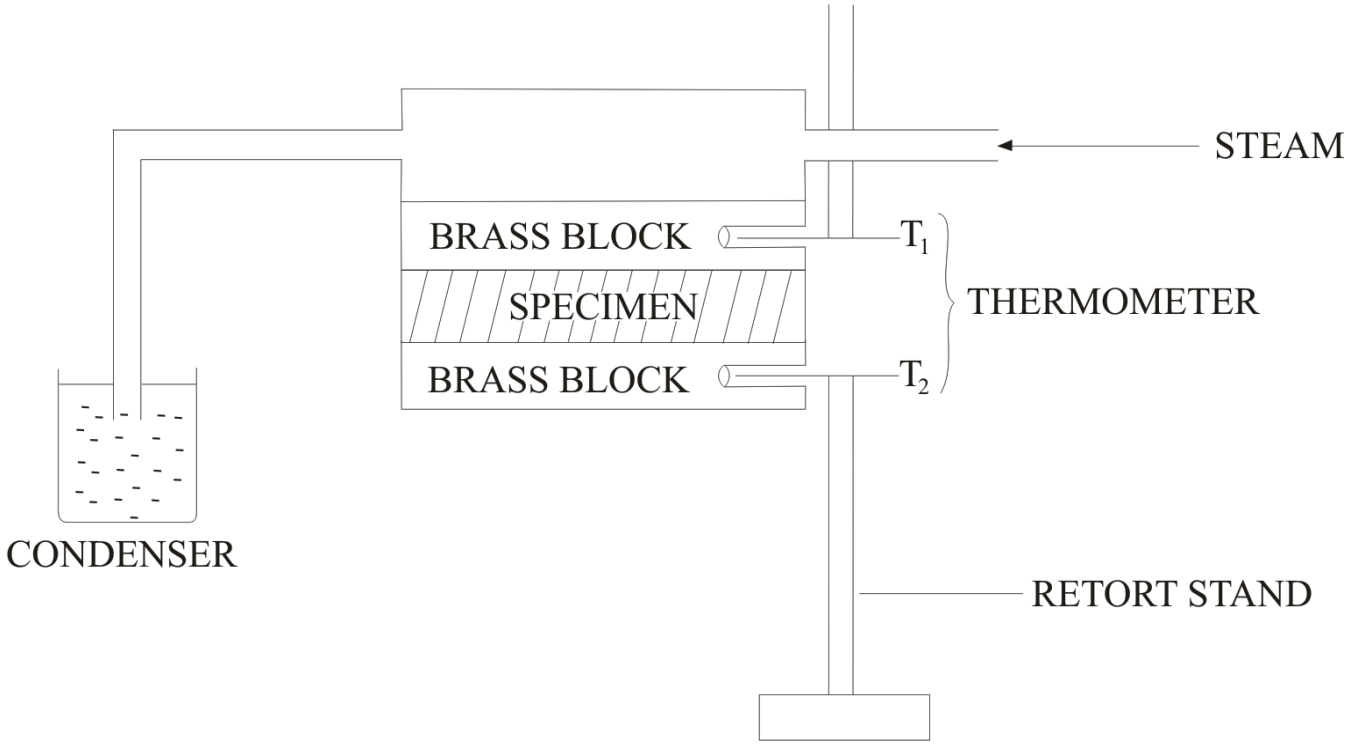


Fig 13: Apparatus for determination of thermal conductivity using Lee's Disc method

Two rectangular specimens were prepared from the graphite samples (A and B). They were compressed using a (300KN) capacity University Testing Machine where extended load was gradually applied until enough to compress the material. The maximum load was no read off the indicator on the machine, and the value divided by the original area of the specimen under test to arrive at the maximum compressive strength in ($N/mm^2$). This is given by the relation

$$Jc = \frac{P_{max}}{A_o}$$

Where JC = compressive strength

$P_{max}$ = maximum load applied

$A_o$= original area of the specimen

Note, $J_{c\ max} = JC$

Where $J_{c\ max}$ = maximum compressive strength, $N/mm^2$

$J_c$=compressive strength, $N/mm^2$

**c) Thermal Shock Resistance (TSR)**

The thermal shock resistance of an undisturbed solid is the ability of that solid substance to withstand heat for a given period of time before failure or deformation is manifested. The apparatuses used for this experiment include refractory bricks, furnace, pair of tongs and two graphite samples.

Test pieces of refractory bricks were thoroughly dried and placed n a cold furnace and heated at a rate of 5ºC/mm up to 1200ºC. The testing temperature was kept for thirty (30) minutes and then the bricks were removed from the furnace with a pair of tongs previously warmed in the furnace for a short time. The graphite test piece was then placed on the cooled fire bricks in a position free from draughts. After the test pieces had been cooled in this way for ten (10) minutes, they were put back into the furnace for another ten (10) minutes. The cycle was repeated thirty (30) times until the failure occurred, indicated by appearance of cracks. The material would be reported to have excellent thermal shock resistance if no crack occurs after three hundred (300) minutes.

In this particular test, none of the two graphite samples experienced failure throughout the duration of the test. In order to test the inertness of the graphite samples, each of them was reacted with 4% $HNO_3$ in methylated spirit. None of the samples was affected by the nitric acid ($HNO_3$) after the test.

Pieces had been cooled in this way for ten (10) minutes; they were put back into the furnace for another ten (10) minutes. The cycle was repeated thirty (30) times the failure occurred indicated by appearance cracks. The material would be reported to have excellent thermal shock resistance if no crack occurs after three hundred (300) minutes.

## 3.3 STRUCTURAL FEATURES

Different rock types and their associated structures form important features in field geology. Some of the principal structural features in the field are joints, which are caused by tectonic stresses resulting from fracturing essentially contemporaneously with the tectonic

activity, residual stresses due to events that happened long before the fracturing, and surface movements such as downhill movements or rockfalls or mountain glaciers (Billings, 1972). Other distinctive structural features in the project area include veins, quartzitic and magmatic dykes, strike-slip faults, and shear zones. Almost all in-situ rock outcrops in the area display different but characteristic joint system. Some of the rocks (such as the granite gneisses) display few joints systems while others are mineralized, while yet others are cross joints, characterized by microfaults. These are shown in Plates 3 – 5. Measurements of the joints are presented on Table 7 and a rose diagram in Fig. 14.

### 3.3.1 Veins

Veins are tabular sheet-like mineral bodies which have intruded vertically into joints or fissures. The veins usually occur along faults or fracture zones in form of mineralization due to the movement of molten materials that solidify along the fractures or faults (Ekwueme, 2003).

Quartz veins occur in muscovite biotite granite (1A) at Walon Kole village, in migmatitic gneiss (2A) in the north-eastern part of the project area and in the south-west within a shear zone. Most of the veins follow direction of the joint which trend NE-SW and SW-NE (Plate 6a, b, c).

Feldspathic veins occur within the biotite granite and trend NW – SE and NE – SW following the direction of foliation (Plates 7 and 8). The veins in the south-eastern part of the area occur in shear faults and are typically layered. The rock units bordering these shear vein system are highly folded such as the simple granitic pegmatitic and amphibolites which host the graphite.

Plate 3

Plate 4

Plate 5 (a and b)

**TABLE 7: STATISTICAL PRESENTATION OF JOINT REDINGS/FOLIATIONS IN THE PROJECT AREA**

| Joint readings taken | Class interval | Frequency of occurrences | Percentage of total | Equivalent Radius (cm) |
|---|---|---|---|---|
| 152, 69, 102, 60(5)<br>165, 64, 3(2), 99(3)<br>153, 14(2), 55(6), 50(4)<br>172, 14(2), 59(2), 163(6)<br>155(3), 48(7), 38(4)<br>166(4), 172(5), 160(4), 172(2), 68(d.65 sw)<br>165(3), 64, 58(6), 62<br>178(2), 169(3), 70(d, 65sw)<br>177, 54, 178(2), 60(2),<br>64(d.65sw), 127(3) 63<br>58(5), 81, 146(2), 123(4),<br>121(4), 96, 86<br>99, 90(4), 137(2), 44, 46, 51 | 0 – 30 | 6 | 5.04 | 0.25 |
| | 31 – 60 | 45 | 37.81 | 1.89 |
| | 61 – 90 | 13 | 10.92 | 0.55 |
| | 91 – 120 | 4 | 3.36 | 0.17 |
| | 121 – 150 | 12 | 10.08 | 0.54 |
| | 150 – 180 | 39 | 32.77 | 1.6 |
| | **TOTAL** | **119** | **99.98** | **5cm** |

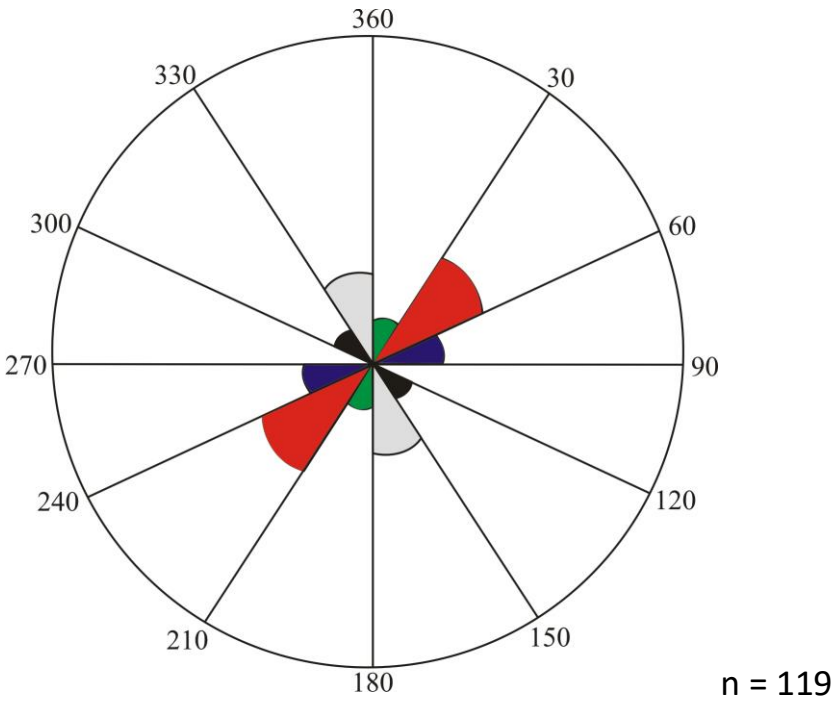


Fig 14: Rose diagram of joint systems in the project area

Plate 6

Plate 7 and 8

### 3.3.2 Faults

Most of the rocks are characterized by microfaults as shown in Plate 7 – 8. Faults are ruptures in which the opposite walls have moved past each other. The movement could be vertical or horizontal but could occur together (Ekwueme, 2003). The most essential feature of faulting is the differential movement which is always parallel to the surface of the fractures (Billings, 1972). The project area has three principal types of faults; strike-slip fault which occur in shear zones in a contact between migmatite, amphibolites and simple granitic pegmatite in the project area, characterized by multiple micro and mega faults as shown in Plate 6; microfaults which occur in joints or foliations as in Plates 7 – 8; and the third type is simple block faulting which is exposed in a stream bordering the graphite zone at Walon Kole (Plate 9, a, b c, d, and 10)

### 3.3.3 Shear Zones

These are zones across which blocks of rocks have been displayed in a fault-like manner but without prominent development of visible faults (Hobbs et al, 1976). The shear zones in the area trend S-W and NE and are associated with strong foliations which are brittle in nature. As pointed out by Roberts and Sheahan (1990), brittle shear zones are characterized by abrupt offsets of markers and associated with faults or breccias following tectonic deformation as can be seen in Plate 6 and 7. In Plate 6, it is evident that the area may have undergone tectonic deformation due to differential shear stresses resulting into faults, lineations, folding, fracturing and shearing. In Plate 8, deformed veins may have been formed earlier as shearing stresses progressed.

Plate 9 (a and b)

Plate 9 (c and d)

Plate 10 (a and b)

### 3.3.4 Folds

Folds describe the distribution of material volume which is manifested as a bend or nest of bends in a linear and planar fashion in the structure which is being folded (Ekwueme, 2003). Many fold systems in the area occur in the south-west and north-east sections of the mapped area. Evidence of strong folding of these rock units is shown by the brittle shear zone in the stream separating these rock units in the south (Plate 6). About two-thirds of the rock units in the area have certain features of folding as manifested by the anticlines and synclines in muscovite-biotite granites, biotite granites, amphiboles and granite-gneisses. The fold system varies but includes open symmetrical folds to the north, tight folds to the south-west and north-central. Manifestation of shear folding in the area is indicated by the shear zone exposed in a stream in the south-west (Plate 6).

### 3.3.5 Dykes

Dykes are tabular bodies of igneous rocks which cut across massive structures of older rock bodies, most of which are formed due to the injection of magma into fracture systems and could be simple, composite, ring, complex and differential (Billings, 1972). Dyke systems mapped in the area include quartzite and pegmatitic. Two prominent quartz dykes occur south, one of Mayo Butale village while another occur in the north-west of the first dyke. Both dykes are simple as they were formed by a single intrusion of magma. The first dyke with steep sides trends NE-SW is about a kilometer in length and 600 metres wide and makes contact with biotite granite (plate 11a) and migmatite while the second dyke located in the north-west is smaller with gentle sides (in 30 – 450), makes contact with muscovite-botite granite and trends NE-SW.

### 3.3.6 Fault Breccias

Breccias are angular to sub-angular rock fragments composed of different sizes and always occur in a matrix of finer material. They are for the most parts associated with fault with the breccias occurring along the plane (Billings, 1972; Weyman, 1981). In the project area, fault breccias occur within a fault zone south of Walon Kole village where graphite (2C) is exposed. Amphibolite rocks hosting the graphite are wholly enclosed by the fault breccias, (Plate 9 a and b). The exploration trench shown in Plate 10 adjoins the amphibolites zone.

### 3.3.7 Horsts and Graben

A horst is a block of rock body whose length is more than its width and which has been raised relative to the blocks on either side; a graben is a block of rock body which is longer than its width that has been lowered relative to the blocks or either side of the rock body (Billings, 1972). The faults bounding the horsts and graben are usually normal faults which for the most part are steep. The graphitic zone in Walon Kole area lies wholly within a fault zone in graben-like (downwarped) structure bounded on each side by fault breccias. The amphibolites hosting the graphite zone are intruded by short and discontinuous quartzitic dykes trending NE-SW. with the granitic rocks which outcrop on either side of the graben structure and in a stream exhibit microfaults. On the basis of these observations, three zones are therefore recognized within the graben structure and these are the graphite zone, the breccia zone and the block horsts as shown on Plate 11 (b c, d, e and f). The width of the graben structure is about 400 metres, and the length is about 1 kilometer). Plate 12 shows Mayo Butale graphite zone with associated structural features.

Plate 11 (a, b and c)

Fig 11 (d and e)

Plate 11f

Plate 12

## 3.4 ECONOMIC GEOLOGY, HYDROGEOLOGY AND WATER RESOURCES

### 3.4.1 Economic Geology

Economic geology aims at discussing the effects of geology on human activities such as mining, agriculture, forest and animal resources, extraction of notable metallic, non-metallic and construction materials and the uses to which these resources may be applied (Ogezi, 1996). Mineralization of graphite and other mineral occurrences in the area promote mining activities, albeit illegally.

Many of the indigenes and other unregistered miners are involved in this act. Other minerals available as occurrences in clued barites, iron ore, silver, tantalite, mercury, radio-active minerals, brick and ceramic clays, copper, feldspar, construction material such as sands, granites, laterites, gravels and gemstones (Plates 13 a and b). These minerals form one of the major natural resources of the area which can be exploited for general development of the area.

### 3.4.2 Hydrogeology and Water Resources

The occurrences of water resources, its extraction, use and chemical quality and quantity define the principal aim of hydrogeology and entail both the surface and underground water potentials of the area. The surface water resources of the area are enormous as shown by the mean annual rainfall (1400 to over 1600mm), mean annual onset dates and mean cessation dates of rains and the mean length of rainy season in Fig 12 (a, b, c, d) (Adebayo and Tukur, 1999). Unfortunately, however, no large resources and dams have been constructed to store the excessive overflows, but the underflow of most of the streams are exploited by the people

Plate 13

Fig. 12: Mean Annual Rainfall

through shallow hand-dug wells during dry periods for drinking, irrigation and livestock.

The groundwater potential of the area can best be described as moderate which can sustain the groundwater needs of the existing population in terms of quality and quantity. These are exploited through construction of shallow boreholes into the thick eluvium and the fractured basement, Plate 14 shows one of such shallow boreholes drilled into thick eluvium in Toungo town. The qualities of the groundwater lie within the recommended limits by the World health Organization (WHO), standards for drinking water.

Plate 14

# CHAPTER FOUR

# DATA PRESENTATION AND DISCUSSION

## 4.1 Data Presentation

Data from all the analyses and determinative tests for all rock samples from the project area are presented in Tables and plots.

### 4.1.1 Chemical Analysis

Tables 8 and 9 show summary results of the elemental contents and oxides of rocks while the computer print details are presented as appendixes 2 (a - j) and 3 (a - h). Appendix 3 (i) and (j) are not computer print but tabulated chemical analysis result from NMDC, Jos, detached chemical analysis result. Elements determined include carbon (C), oxygen (O), sodium (Na), magnesium (Mg), aluminium (Al), silica (Si), zirconium (Zr), sulphur (S), chlorine (Cl), potassium (K),titanium (Ti), vanadium (V), chromium (Cr), manganese (Mn), iron (Fe), nickel (Ni), copper (Cu), and zinc (Zn). The elemental components were first determined while their oxides were computed from empirical formula.

Fig 16 (a – n) also shows differentiation Index DI = 1/3 (Si + K) – (Ca + Mg) graphs of Nockolds and Allen (1953) while Fig 17 shows Harker plots where oxides are plotted against silica content (Rollinson, 1993); Fig 18 shows Alkali – Sililca diagram of Irvine and Baragar (1971), Fig. 19 shows carbon plots of the rocks in the area and Fig. 20 shows chemical variation diagram for the rocks.

Table 8

**TABLE 9 CHEMICAL COMPOSITIONS (OXIDES) OF ROCKS FROM THE PROJECT AREA: THEIR RATIOS, RANGES, AVERAGES AND DI VALUES**

| S/N | Elements/ Oxides | Alkaline Rocks | | | Migmatite – gneiss complex | | | | Graphitic rock | | Amphi bolite |
|---|---|---|---|---|---|---|---|---|---|---|---|
| | | 1A | 1C | 1D | 2A | 2B | 7 | 8 | 1B | 2C | 9 |
| 1. | $SiO_2$ | 52.11 | 33.58 | 80.42 | 44.73 | 34.53 | 29.69 | 52.11 | 52.41 | 71.26 | 0.47 |
| 2. | $TiO_2$ | 1.23 | 2.38 | 0.35 | 0.18 | 1.07 | 4.78 | 0.66 | 0.93 | 1.79 | 2.40 |
| 3. | $Al_2O_3$ | 16.86 | 13.98 | 10.40 | 15.86 | 14.08 | 14.29 | 13.23 | 24.92 | 18.61 | 6.18 |
| 4. | $Fe_2O_3$ | 7.95 | 43.37 | 6.54 | 2.10 | 20.17 | 36.70 | 8.17 | 1.11 | 3.48 | 40.15 |
| 5. | MnO | 0.35 | 0.68 | ND | 0.36 | 0.36 | 0.10 | 0.42 | 0.19 | ND | ND |
| 6. | MgO | 0.02 | 1.73 | ND | 0.13 | 0.91 | 0.53 | ND | 0.31 | 0.16 | 0.65 |
| 7. | CaO | 4.93 | 2.74 | 1.23 | 3.78 | 26.82 | 4.53 | 7.80 | 1.66 | 2.16 | 39.31 |
| 8. | $Na_2O$ | 0.79 | 0.47 | 0.29 | 0.42 | 0.68 | ND | 0.70 | 0.13 | 0.01 | 0.14 |
| 9. | $K_2O$ | 16.69 | 1.32 | 2.24 | 33.55 | 1.85 | 10.40 | 17.85 | 18.30 | 2.85 | 1.91 |
| 10. | $P_2O_5$ | ND | ND | ND | ND | ND | ND | ND | ND | ND | ND |
| 11. | $Cr_2O_3$ | 0.03 | ND | ND | 0.21 | -0.03 | 0.39 | ND | 0.36 | 0.52 | -0.03 |
| 12. | CuO | 0.38 | 0.98 | 0.50 | 0.02 | 0.36 | 0.36 | 0.07 | 0.92 | 0.59 | 0.17 |
| 13. | ZnO | 0.18 | 0.25 | 0.58 | 0.49 | 0.04 | ND | ND | 0.35 | 0.69 | 0.44 |
| 14. | $SO_2$ | 0.08 | 1.14 | 0.11 | 0.09 | 0.02 | 0.08 | 0.00 | 0.11 | 0.07 | 0.14 |
| 15. | C | ND | 0.75 | 0.06 | ND | ND | 0.62 | ND | 0.82 | 3.0 | 0.47 |
| 16. | Ni | 0.07 | ND | 0.16 | 0.10 | ND | ND | 0.10 | 0.22 | ND | 0.18 |
| 17. | Cl | 0.05 | ND | ND | 0.03 | 0.07 | 0.11 | 0.10 | ND | 0.05 | ND |
| **Total** | | 101.25 | 101.99 | 101.98 | 101.96 | 101.34 | 101.96 | 101.77 | 100.67 | 100.11 | 100.82 |
| Ratio | $K_2O/Na_2O$ | 21.11 | 2.75 | 7.72 | 79.8 | 2.72 | ND | 25.50 | 140.76 | 285.0 | ND |
| 2 | $TiO_2/Al_2O_3$ | 0.07 | 0.17 | 0.03 | 0.01 | 0.07 | 0.35 | 0.03 | 0.03 | 0.09 | 0.35 |
| 3 | $Na_2O + K_2O$ | 17.48 | 1.79 | 2.53 | 33.97 | 2.53 | 10.46 | 18.55 | 18.43 | 2.86 | 2.05 |
| 4 | $Al_2O_3/Na_2O$ | 21.34 | 29.74 | 35.86 | 37.76 | 20.71 | ND | 18.90 | ND | 1861.0 | 44.14 |
| 5 | DI | 11.23 | 19.11 | 13.34 | 16.28 | 15.04 | 4.58 | 8.45 | 14.92 | 10.41 | 16.47 |
| 1 | $SiO_2$ range | 33.58 to 80.42 | | | 29.69 to 52.69 | | | | 52.41 to 71.26 | | |
| 2 | $TiO_2$ range | 0.35 to 2.38 | | | 0.18 to 4.78 | | | | 0.93 to 1.79 | | |
| 3 | $Na_2O$ range | 0.29 to 0.79 | | | 0.0 – 0.70 | | | | 0.01 to 0.13 | | |
| 4 | $Na_2O$ Average | 0.71 | | | 0.43 | | | | 0.07 | | 0.14 |
| 5 | $K_2O$ range | 1.32 to 16.69 | | | 1.85 to 33.55 | | | | 2.85 to 18.30 | | |
| 6 | $K_2O$ Average | 6.77 | | | 15.91 | | | | 10.57 | | 1.91 |
| 7 | $Al_2O_3$ range | 10.40 to 16.86 | | | 13.23 to 15.86 | | | | 18.61 to 24.92 | | |
| 8 | $Al_2O_3$ Avg | 13.76 | | | 14.34 | | | | 21.76 | | 6.18 |

Key

1A: Muscovite biotite granite

1C: Biotite granite

1D: Simple granitic pegmatite

2A: Migmatitic gneiss

2B: Migmatite

7: Granite

8: Pyroxene-rich gneiss

ND: Not detected

DI: Differentiation index

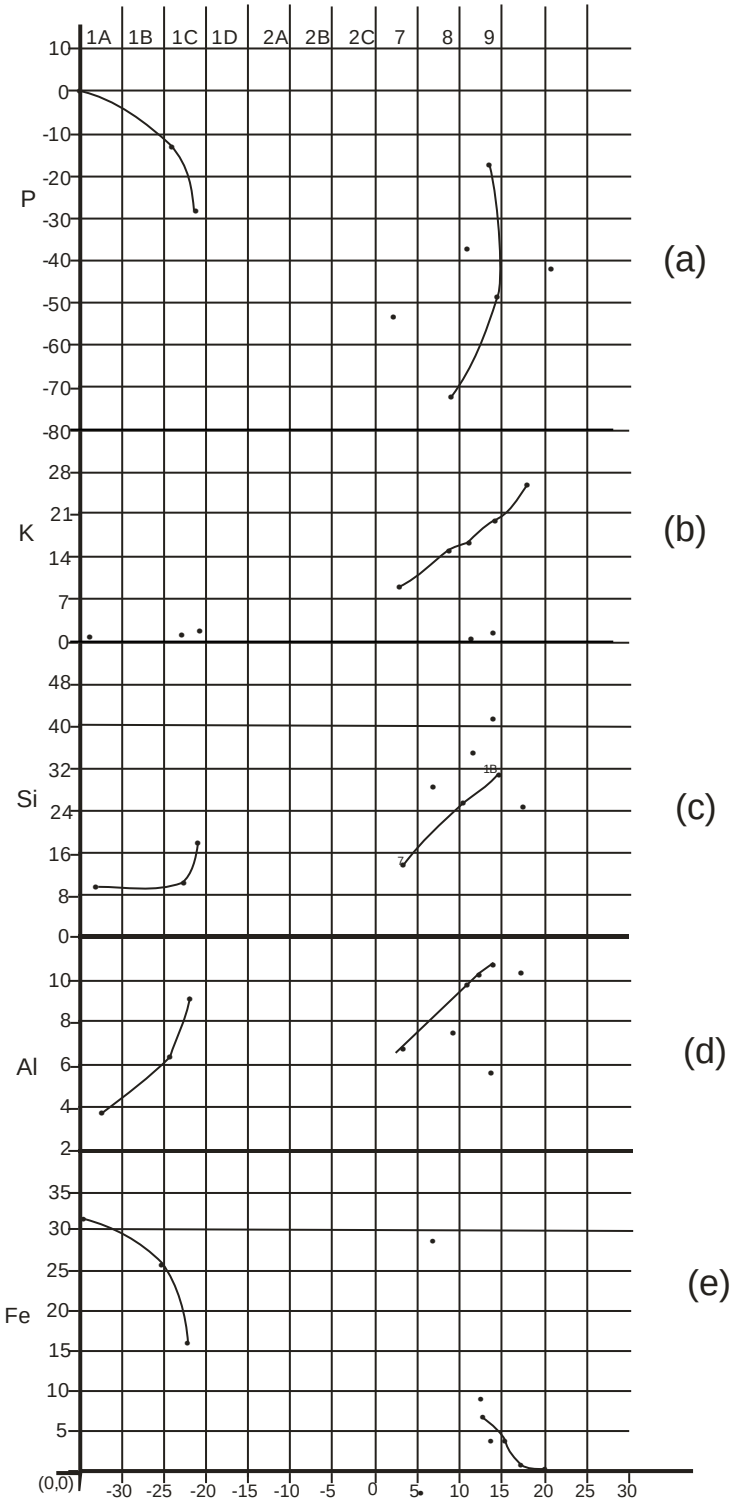


DI = 1/3 (Si + k) - (Ca + Mg)

Fig. 16: (a - n): Differentiation Index (DI) plots for rocks of the project area

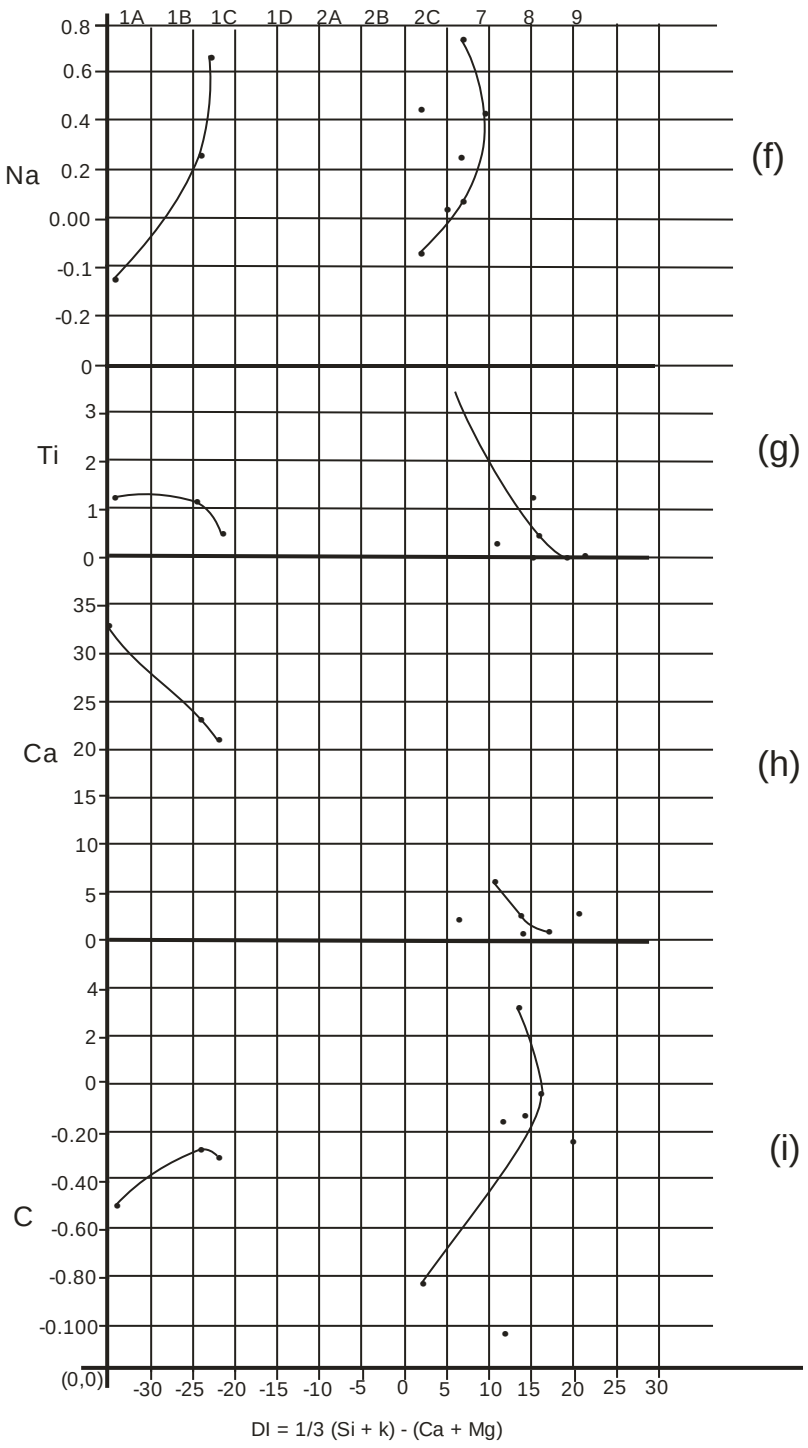
1A 1B 1C 1D 2A 2B 2C 7 8 9
Na
Ti
Ca
C
(f)
(g)
(h)
(i)
0.8 0.6 0.4 0.2 0.00 -0.1 -0.2 0
3 2 1 0
35 30 25 20 15 10 5 0
4 2 0 -0.20 -0.40 -0.60 -0.80 -0.100
(0,0)
-30 -25 -20 -15 -10 -5 0 5 10 15 20 25 30
DI = 1/3 (Si + k) - (Ca + Mg)

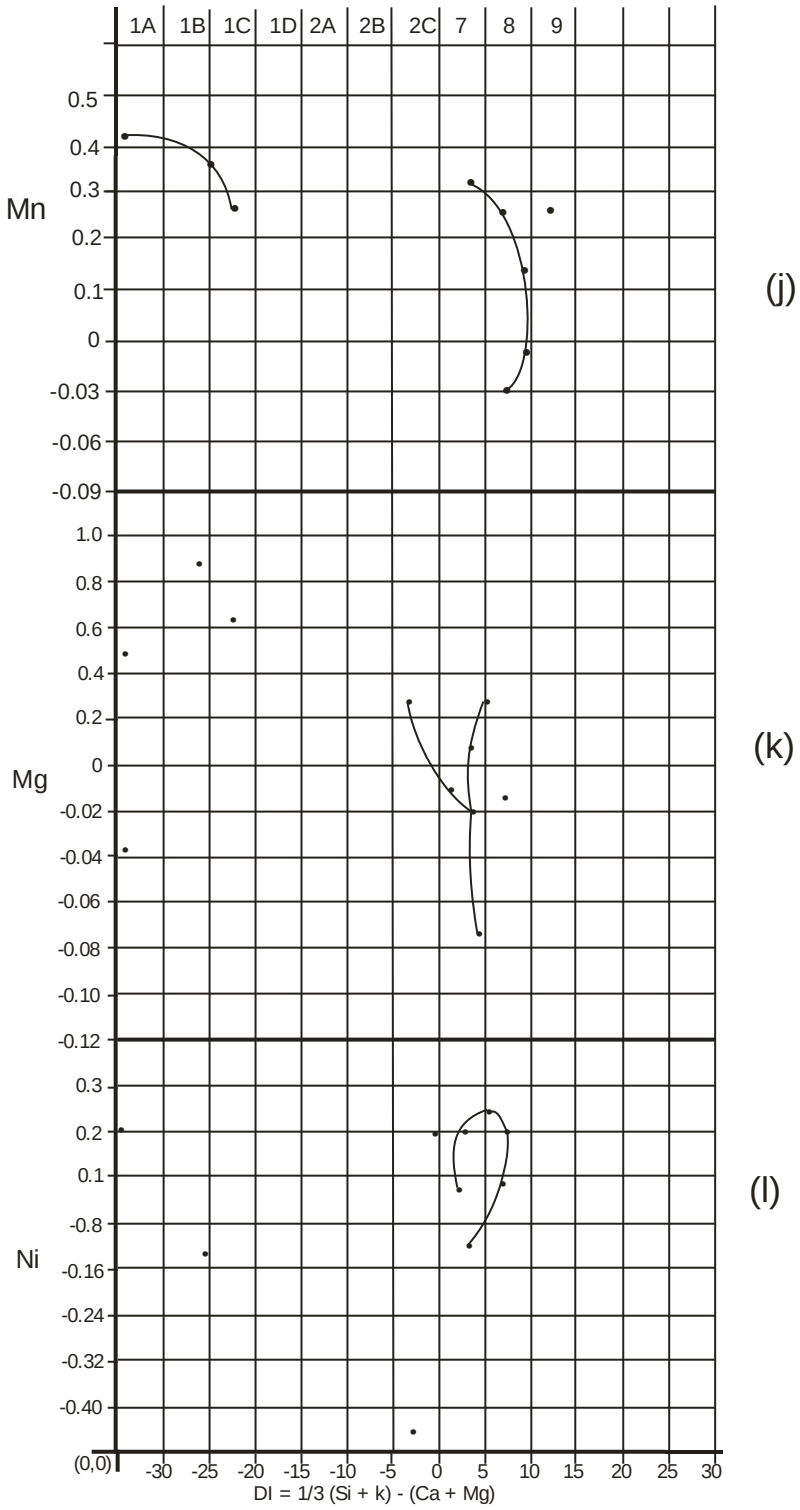
1A
1B
1C
1D
2A
2B
2C
7
8
9
Mn
0.5
0.4
0.3
0.2
0.1
0
-0.03
-0.06
-0.09
(j)
Mg
1.0
0.8
0.6
0.4
0.2
0
-0.02
-0.04
-0.06
-0.08
-0.10
-0.12
(k)
Ni
0.3
0.2
0.1
-0.8
-0.16
-0.24
-0.32
-0.40
(l)
(0,0)
-30 -25 -20 -15 -10 -5 0 5 10 15 20 25 30
DI = 1/3 (Si + k) - (Ca + Mg)

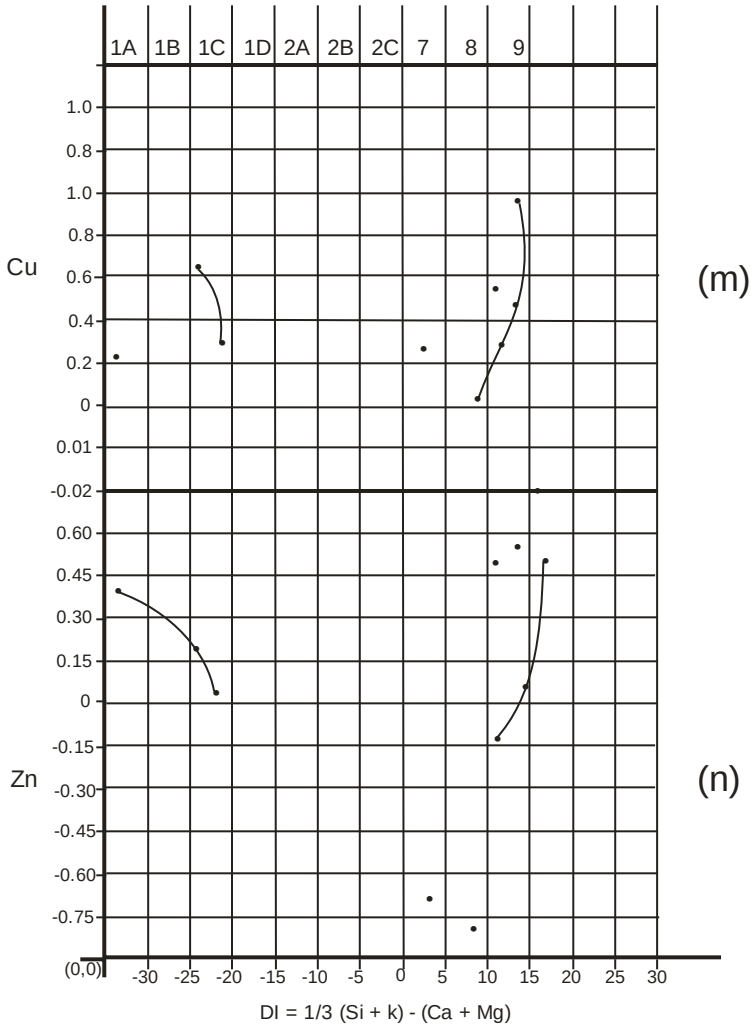
1A
1B
1C
1D
2A
2B
2C
7
8
9
1.0
0.8
1.0
0.8
Cu
0.6
(m)
0.4
0.2
0
0.01
-0.02
0.60
0.45
0.30
0.15
0
-0.15
Zn
-0.30
(n)
-0.45
-0.60
-0.75
(0,0)
-30
-25
-20
-15
-10
-5
0
5
10
15
20
25
30
DI = 1/3 (Si + k) - (Ca + Mg)

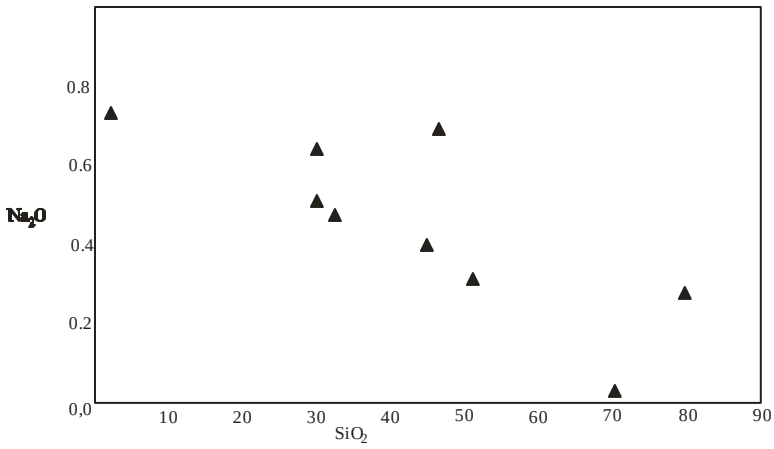


(a)

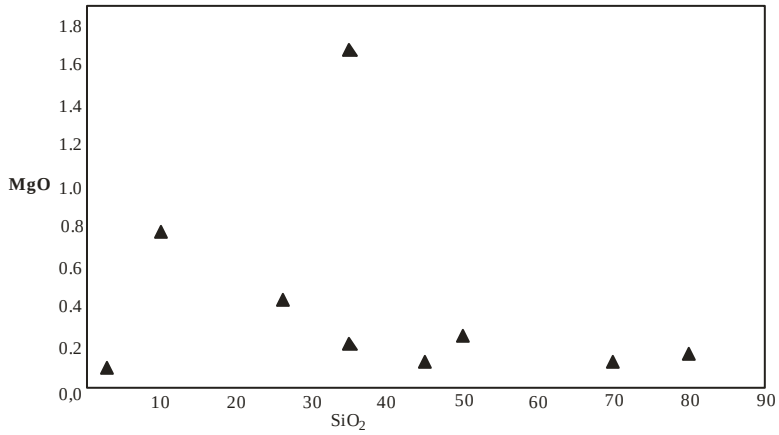


(b)

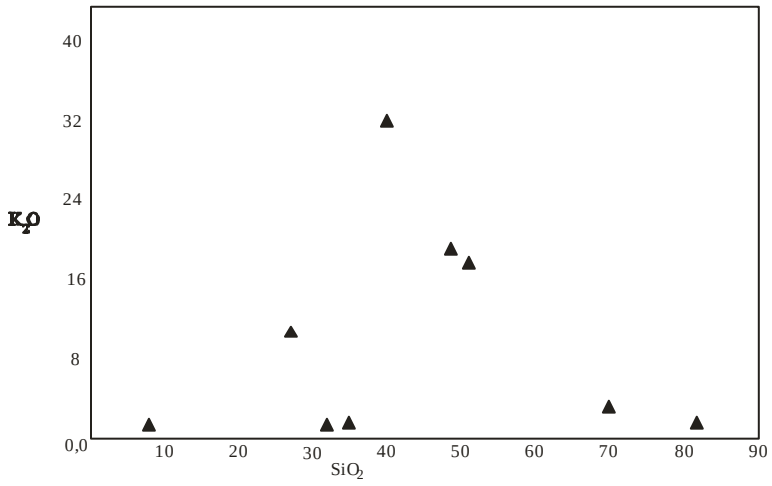


(c)

**Fig 17 (a - g): Harker Variation plots for rocks of the project area**

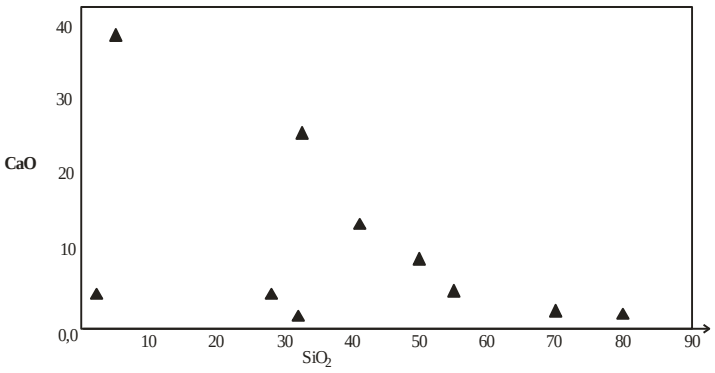
CaO
40
30
20
10
0,0
10 20 30 40 50 60 70 80 90
SiO2

(d)

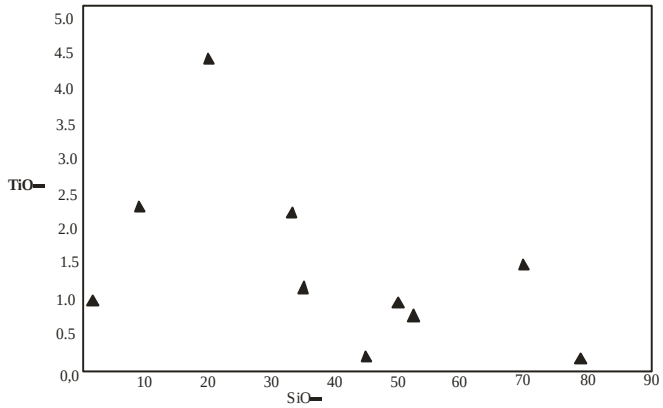
TiO
5.0
4.5
4.0
3.5
3.0
2.5
2.0
1.5
1.0
0.5
0,0
10 20 30 40 50 60 70 80 90
SiO

(e)

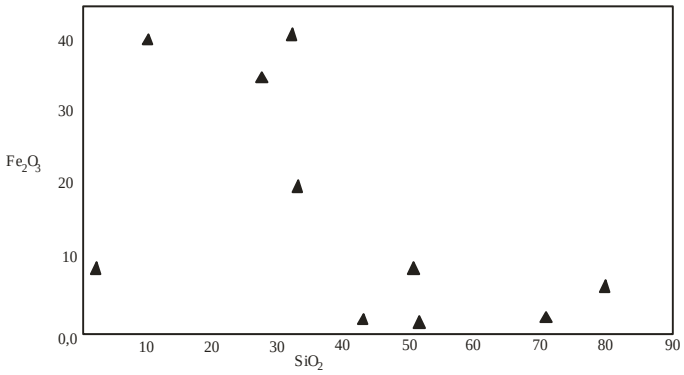
Fe2O3
40
30
20
10
0,0
10 20 30 40 50 60 70 80 90
SiO2

(f)

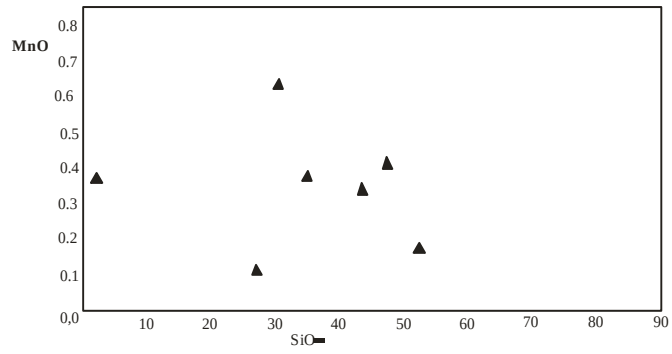
MnO
0.8
0.7
0.6
0.5
0.4
0.3
0.2
0.1
0,0
10 20 30 40 50 60 70 80 90
SiO

(g)

>

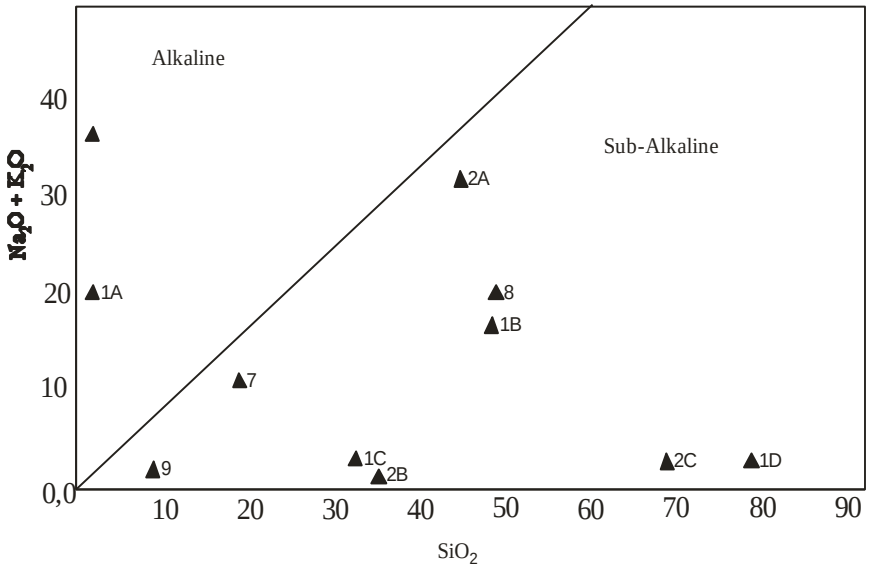


Fig 18: Alkali-Silica discrimination diagram for rocks from the project area

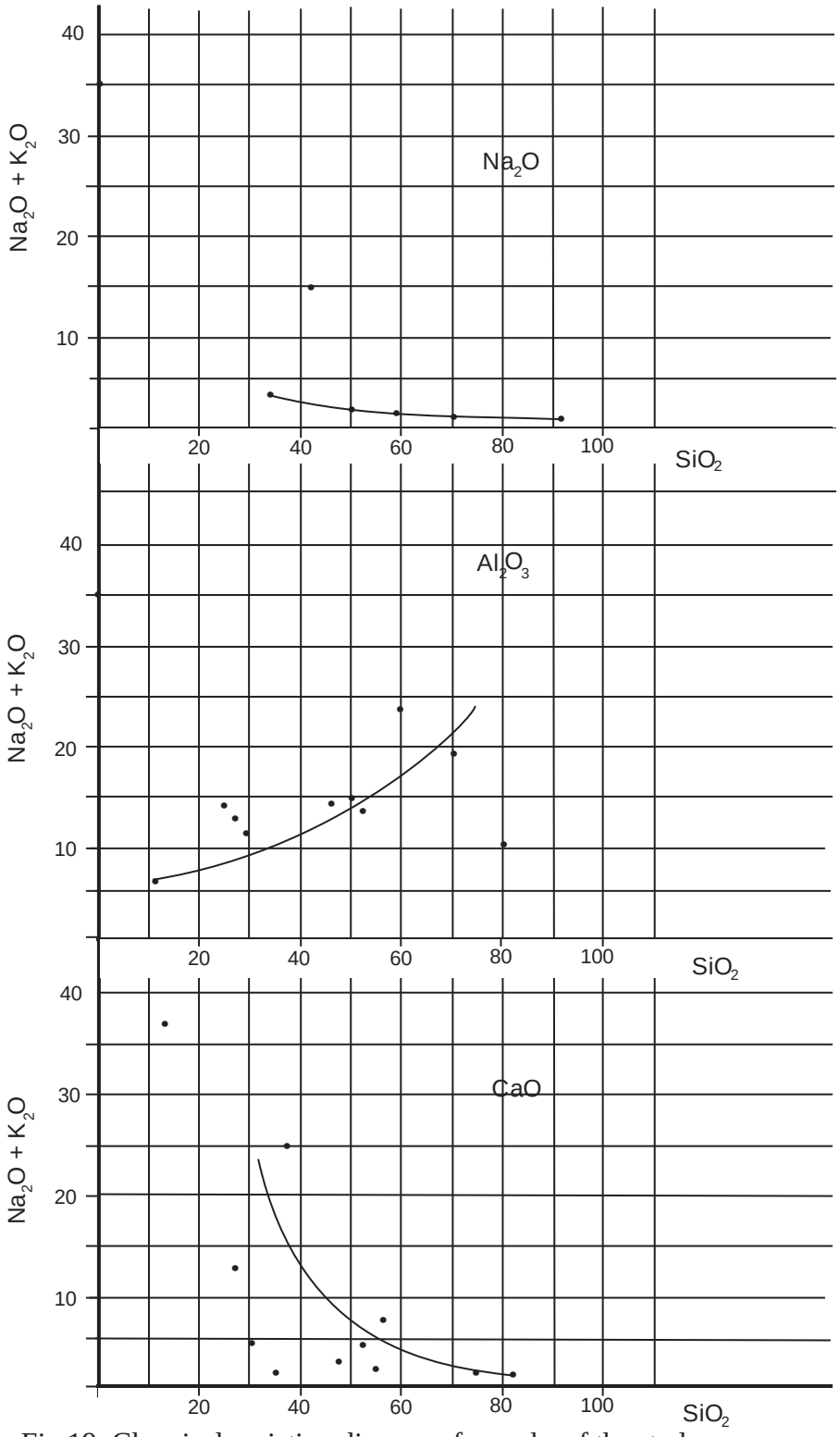

Fig 19: Chemical variation diagrams for rocks of the study area

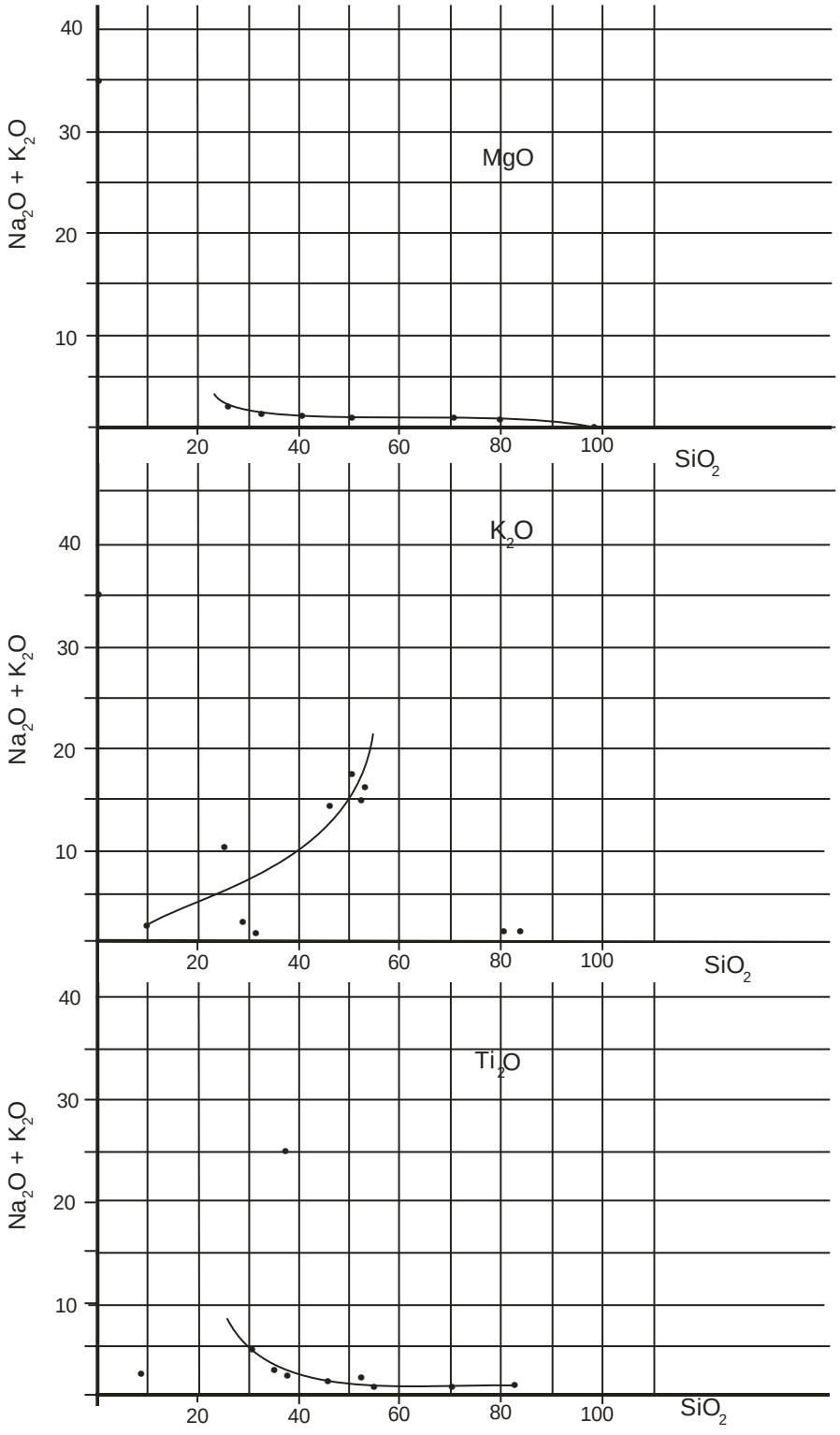
40
30
20
10
$Na_2O + K_2O$
MgO
20
40
60
80
100
$SiO_2$
$K_2O$
$Ti_2O$

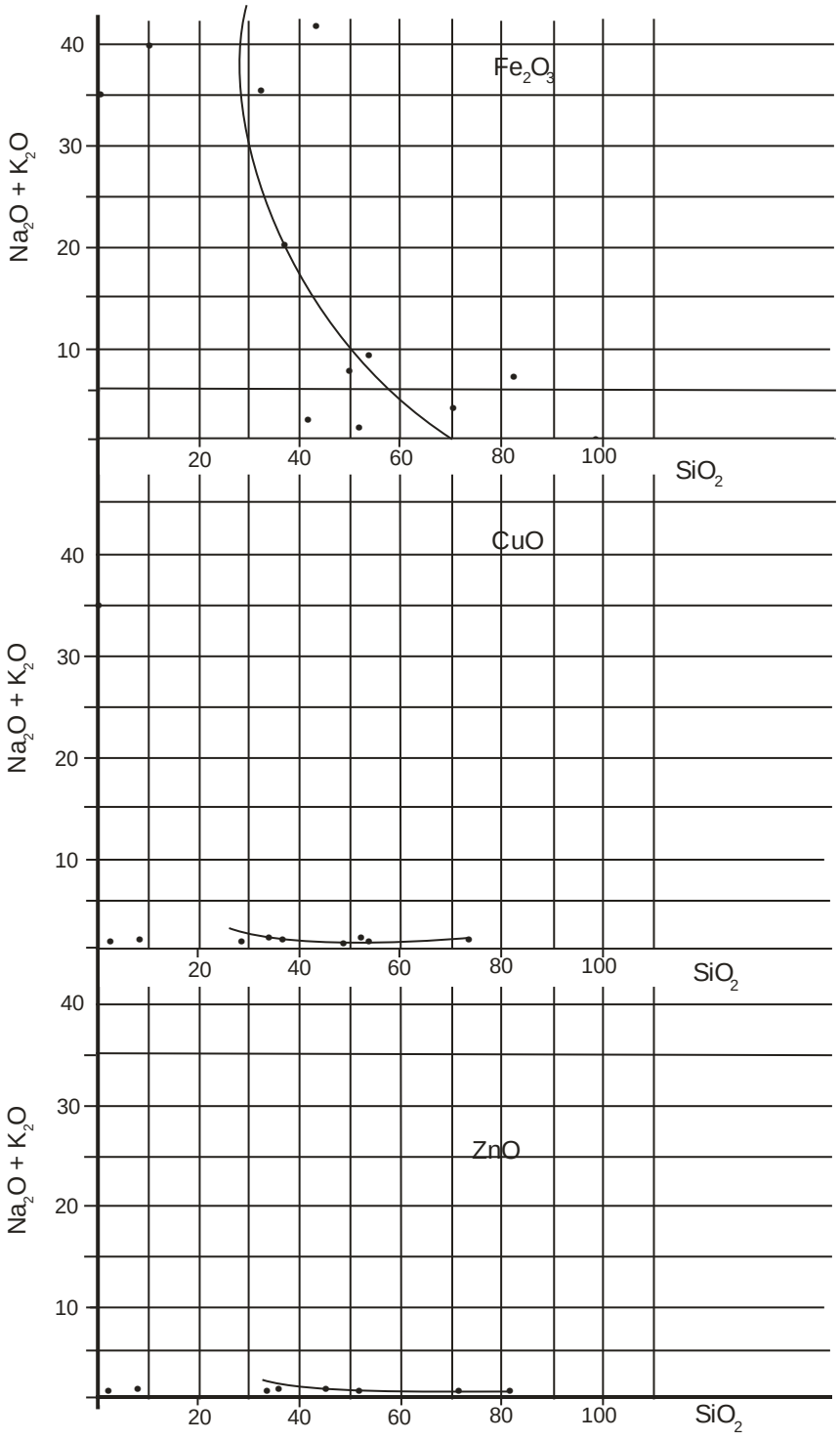
Fe2O3
CuO
ZnO
Na2O + K2O
SiO2
10
20
30
40
20
40
60
80
100

### 4.1.2 Petrographic Studies

A total of 38 thin sections from ten different samples were studied in details and the rocks identified. The samples are 1A, 1B, 1C, 1D, 2A, 2B, 2C, 7, 8 and 9. The slides were examined at two centers; The Nigerian Metallurgical Development Centre, Jos and at the Geology Department, University of Jos. At both laboratories, the microscopes are fitted with photo-micro graphic facilities. Photomicrographs of the studied samples are presented in Appendix 8.

#### 4.1.2.1 Sample 1A

In hand specimen, the rock is light coloured, hollocrystalline, medium to coarse-grained with visible quartz grains and feldspar phenocrysts. Biotite and muscovite micas appeared as black shiny flakes and white shiny particles respectively as was confirmed with a X12 hand lens.

In thin section, the rock was examined under magnification of 32 and 100 and shows quartz with sutured boundaries dominating the slide (Appendix A8 – 1). They equally show undulose extinction. Some of the grains have inclusions (vacoules) while others have straight boundaries with straight extinction. The presence of sutured boundaries and undulose extinction suggest high stress on this rock. Texturally, most of the quartz in this rock have fractures with micaceous material filling the spaces. The feldspars present include plagioclase which can be distinguished by its multiple twinning; microcline showing cross-hatch twinning and orthoclase with single twinning. Most of these minerals have been affected by weathering as they show alterations on their surfaces to clay minerals. Biotite in the rock occurs as short tabular brownish crystals.

Modal analysis of the rock shows the following:

| | |
|---|---|
| Orthoclase feldspar | 14% |
| Plagioclase feldspar | 19% |
| Quartz | 33% |
| Microcline | 23% |
| Biotite | 6% |
| Muscovite | 4% |

Accessories (possibly magnetite, oligoclase, sphene, etc) = 1% for all rock samples are presented as Appendix 4 (a - z)

As the rock is light-coloured, hollocrystalline, contains feldspar, quartz and mica, it is plutonic acid igneous rock possibly granite; and due to its biotite content, forming the principal accessory component, it is biotite granite. As the biotite content exceeds that of muscovite, it is muscovite-biotite granite which may have cooled slowly under conditions of low temperature and pressure from an igneous melt. This rock type occupies almost one – fifth of the total areal extent of the project area and is found in two areas to the South-East and North-Central portions of the project area. Most of the rock is characterized by steep slopes and rise from about 610 meters to 930 meters above sea level. In the South – East, they form a long structure while in the North-Central; they form ridge-like structures and rise from 244 meters to 793 meters and are characterized by sharp and steep anticlines 10 - 15°.

#### 4.1.2.2 Sample 1B

In hand specimen, the rock is pinkish with a metallic luster, greasy, soft, fine-grained and scaly. It has shiny micaceous particles and carbonic substances.

In thin section, the rock was examined under magnification of 32 and 100. This rock is composed of quartz, which is colourless with low relief and no cleavage. The quartz has straight to sutured boundaries with slightly undulose extinction (Appendix A8 – 2). Biotite in the sample displays a characteristic one directional cleavage with parallel extinction and looks yellowish to reddish – brownish. There are lots of pale-green micas (muscovite) and needle-like opaque flakes of graphite most of which are embedded in foliated granitic rock as shown in Appendix A8 – 2a. The micas and the graphite are concentrated at the base of Appendix A8 – 2b. They occur as parallel flakes trending towards the direction of foliation.

The approximate modal analysis of the rock shows the following:

| | |
|---|---|
| Quartz | 51% |
| Micas | 21% |
| Graphitic feldspar | 26% |
| Accessories | 2% |

As the rock contains quartz and mica, it is a granitic rock. As it contains graphitic flakes with metallic luster, greasy feel, smudges the hand on slightest touch, it is graphite, embedded in a foliated rock possibly schistose or gneissic rock or amphibolites. The graphite occur as flakes in feldspathic micaceous gneiss and presented in a thin layers probably as vein deposits in fractures in country rocks trending in NE – SW directions as observed in the field. In the project

area, the graphitic rocks occur on South – Eastern end of an amphibolites hill which makes contact with a migmatitic gneiss further to the South – East. It forms part of the amphibolites hill which makes contact with migmatitic gneiss to the North and South.

#### 4.1.2.3 Sample 1C

In hand specimen, the rock is light coloured, hollocrystalline, brownish, fine-medium-grained leucocratic (colour index, about 15 – 20), quartz and feldspars which measure about 1.5 – 2cm respectively are easily identified. Biotite micas are also identified as black specks and insignificant appearances of tiny white specks which could be magnetite, oligoclase, etc.

In thin section, the rock was examined under magnification of 32 and 100 (A8 – 3). Quartz has low relief, is colourless, anhedral with wavy extinction due to partial deformation. It has no cleavage. Biotite mica exhibits parallel extinction; the colour is brownish with tabular crystals on the cleavage surface. Plagioclase feldspars show albite twinning due to the high amount of albite; Orthoclase feldspars have low relief, parallel extinction; two cleavages face and are colourless.

Modal composition of each mineral in the sample is given as

Feldspar = 32

Quartz = 41

Biotite = 25

Others-magnetite, sphene, etc 2%

The mineral has quartz, feldspar and mica, which means that it is plutonic, granitic and acid igneous rock. As it has more quartz content than Biotite (which is the principal accessory mineral), it is Biotite granite. This is evidenced by the results of chemical analysis, where silica (131.41) and alumina (6.33) are high (Appendix 4b). This rock might have been formed at about 300°C; crystallization must have been slow due to the hollocrystalline nature of the grains. This rock type outcrops in two areas of the project, i.e. in the North – East and Centre. It is the most extensive of the rocks of the project area and makes about one-third of the total areal extent. It rises from about 1650ft (503 meters) in the South-East to about 2750ft (838 meters), North-West of Wakiri Jalo village. It deeps gently in the South – West (20 - 45°), but steeply-dipping in the North – East from 10 - 25°.

#### 4.1.2.4 Sample 1D

In hand specimen, the rock is light coloured, hollocrystalline, light-brownish, fine-medium grained leucrocratic, with clearly visible quartz and feldspar grains measuring from 0.5 – 1.5cm. There are tiny and minute crystals of black and shiny biotite micas while muscovite, magnetite and other minerals are almost insignificant.

In thin section, the specimen was observed under magnification of 32 and 100 (A8 – 4). The rock is a coarse – grained composed of quartz, biotite and feldspar. The quartz are anhedral with lots of fractions, some have undulose extinction. The quartz has low relief, is colourless and with no cleavage; some of the quartz have straight boundaries with enclosures. The feldspars are mostly plagioclase (typified by albite twinning) and orthoclase showing parallel extinction, two cleavage faces, low relief and cloudy due to alteration. Large subhedral microcline crystals are

also visibly present showing cross-hatch twinning under cross-polars. There are other dark minerals which could be muscovite, garnet, oligoclase and tourmaline. The biotite in the rock is flaky, with brownish granular crystals exhibiting parallel extinction.

The specimen has the following approximate modal composition:

| | |
|---|---|
| Felspar (confined) | 60% |
| Quartz | 28% |
| Biotite | 8% |
| Garnet and Others | 4% |

Because of the high feldspars, quartz and mica, the rock is granitic and acidic igneous rock by the presence of microcline (potash feldspar); while the oligoclase, muscovite, garnet and tourmaline as accessories denote that the rock is a simple granitic pegmatite (Nockolds *et al* 1979). It might have been formed in a deep-seated condition at temperatures of about 300°C as a result of metamorphic differentiation or one short period of igneous activity.

This rock type occurs in the central part of the project area trending NE – SW, with muscovite Biotite granites to the North and further with biotite granites and amphibolites to the North – East. The rock forms about one-sixth of the total areal extent of the project area.

#### 4.1.2.5 Sample 2A

In hand specimen, the rock is fine-medium-grained (hollocrystalline) dark-coloured ferromagnesium rock, colour index 30 – 50, and exhibiting bands with foliations. Feldspars, quartz and micas are clearly discernible with the naked eye. The feldspars are by far less than the ferromagnesians in the rock.

In thin section, rock was examined under magnification of 100 as shown in Appendix A8 – 5. The rock contains prismatic plagioclase feldspars, anhedral to subhedral quartz, and mafic minerals most of which are pyroxenes, biotite, micas and a few grains of olivine. Most of the feldspars are being foliated with smaller grains of them being enclosed in pyroxene and olivine. The biotites are mostly green biotite occurring as tabular crystals. The leucocratic and melanocratic bands give another characteristic feature of this rock. The approximate volume percent of the constituent minerals are as follows:

| | |
|---|---|
| Biotite | 36% |
| Plagioclase feldspar | 25% |
| Quartz | 15% |
| Pyroxene | 10% |
| Olivine | 9% |
| Accessories (sphene, etc) | 5% |

The rock has feldspars, quartz and mica, which means that it, has been of granitic origin, and because it has leucocratic and melanocratic bands, it may be a metamorphosed granitoid, typical by of migmatite due to foliation and parralled bands. As the rock contains more biotite micas than quartz and plagioclase, it may be termed migmatitic gneiss formed due to high-grade regional metamorphic differentiation by partial melting of pre-existing rocks under high temperature, high pressure, and extremely high heat and at depths. The migmatitic gneiss occurs as small rock unit in the South-Eastern part of the project area, making contact with the granite-gneiss. It is gently dipping from 30 – 40 to the South-East. It rises from 579 – 762meters above mean sea level.

#### 4.1.2.6 Sample 2B

In hand specimen, the rock is medium to coarse-grained hollocrystalline. It shows leucocratic and melanocratic bands with colour index of 30 – 50, and highly foliated. It is a dark rock with white colouration set exhibiting parallel bands. Quartz, feldspars and some ferromagnesian can be seen with the unaided eye. The rock was examined under magnification of 32 and 100 and contains the following principal minerals; plagioclase, feldspar, quartz, amphiboles, olivine, pyroxene and biotite micas. The plagioclase occurs in form of prismatic crystals with polysynthetic twinning. The quartz occurs as subhedral grains while the amphibole shows prismatic forms with two cleavage directions. The olivine, pyroxene and biotite occur as fractured and foliated crystals as shown in Appendix 8 – 6.

The rock has the following volume of mineral assemblages:

Plagioclase feldspar 36%

| | |
|---|---|
| Biotite micas | 21% |
| Quartz | 12% |
| Amphiboles | 11% |
| Pyroxene | 9% |
| Olivine | 7% |
| Accessories | 4% |

The rock contains feldspar and quartz which means that it has been of granitic origin, and because it has leucocratic and melanocratic bands, it may be termed metamorphosed granitoid typical of migmatite due to the foliation and parallel bands. The rock may have formed as a result of regional metamorphic differentiation by partial melting of prex-existing rocks under high temperature, possibly 900°C with pressure of up to 12 – 13kilobars and extreme heat at great depth of about 30 – 40km This rock unit occurs as a small outcrop enclosed by an amphibole in the East-Central parts of the project area as could be seen on the geologic map.

#### 4.1.2.7 Sample 2C

In hand specimen, the rock is light-coloured leucocratic, colour index 10-15, pinkish with a metallic lustre. It has a greasy feel with soft and shiny micaceous particles. It is fine-grained and scaly. It smudges the hand as one picks it. It has smooth surfaces with minor undulations. In thin section the rock was examined under magnification of 32 and 100 and found to contain mainly quartz and mica. Quartz is colourlesss, has low relief and no cleavage, and the crystals

are anhedral and elongated following the foliation trend. It has undulose extinction as shown on Appendix A8 – 7. They have straight and sutured boundaries and some of the grains appear as large phenocrysts (1.5-2cm) probably due to recrystallization. The pale-green micas are muscovite. The opaque mineral in the photomicrograph that appear as dark, needle-like flakes is graphite and is mostly associated with muscovite mica.The mineral is embedded in a foliated groundmass. They also appear as laths trending towards the direction of foliation. The rock has the following volume of mineral assemblages:

| | |
|---|---|
| Quartz | 44% |
| Micas | 37% |
| Graphite flakes | 14% |
| Accessories | 5% |

As the rock contains quartz and mica, it is granitic in origin. As it also contains graphite flakes, it is a graphitic rock. As it is characterized by unidirectional cleavage and schistocity with parallel extinction, it is graphite which might have been affected by progressive regional metamorphism through partial melting of the pre-existing rocks under high temperatures possibly below the surface.

The graphite occurs in a fault zone which trends NE-SW and bounded on either side by fault breccias and, block horsts. The graphitic rocks are hosted by amphibolites. These rock bodies lie in Walon Kole valley which has been downwarped forming a graben-like structure characterized by steep-sided fault breccias and block horsts (Plate 13).

#### 4.1.2.8 Sample 7

In hand specimen, the rock has various colours whitish, dark brownish (colour index 25-35), medium to coarse grained, hollocrystalline. It has a gneissose structure characterized by an ill-defined band of leucocratic and mesocratic layers of equigranular and allotriomorphic crystals. In thin section, the rock was examined under magnification of 32 and 100. The rock shows large orthoclase phenocrysts under magnification of 10 Appendix A8 – 8 enclosing foliated biotite crystals in fractures of perthitic orthoclase. The biotite varies from green to brownish pleochroic, one cleavage; the degree of distortion is shown by alteration to chlorite. The quartz in the rock has dotted inclusions with vacuoles and bubbles with few showing unduclose extinction while the plagioclase feldspars are relatively free from alteration, the orthoclase are substantially altered. The feldspars have two cleavages, and parallel extinction with simple twining Garnet crystals are also seen appearing dark under cross polars showing polygonal grains with inclusions as shown in Appendix A8 – 8c and d. The rock has the following mineral assemblages by volume:

| | |
|---|---|
| Quartz | 47% |
| Feldspars | 22% |
| Biotitec mica | 28% |
| Garnet and accessories | 3% |

As the rock has feldspars, quartz and mica it is granitic in origin. As it shows foliated bands of orthoclase feldspars and biotite, it is possibly a metamorphosed granitic rock. The presence of leucocratic and melanocratic bands gives it a gneissic colour. The rock is granite

gneiss formed as result of low grade metamorphism. The rock out crops in the eastern extreme of the project area as ridge-like structure, known as Gudaru Hill. It is steeply-dipping on the southern side (15-19°) but gently-dipping in the north (30 – 45°).

#### 4.1.2.9 Sample 8

In hand specimen, the rock is fine-grained holohyaline, almost melanocratic (colour index 60-75) with feldspars and mica flakes quite visible with a hand lens. In thin section; the rock was examined under a magnification of 32 (Appendix A8 – 9a and b) and 100 (Appendix A8 – 9c and d). The rock shows anhedral olivine, large crystals of pyroxene, biotite, quartz and plagioclase feldspars. The plagioclase feldspars are shown as small prismatic crystals, while the quartz are anhedral to sub-hedral with well-defined boundaries. The pyroxenes and plagioclase feldspar show multiple twining. The rock has the following approximate modal composition.

| | |
|---|---|
| Quartz | 32% |
| Plagioclose felds | 30% |
| Biotite Mica | 25% |
| Pyroxene | 8% |
| Olivine | 4% |
| Others (Ferromagnesians) | 1% |

The rock is quartzofeldspathic as it contains quartz, feldspars, mica and mafic minerals. It is therefore an igneous rock and of granitic origin. As it is dark-coloured with olivine and pyroxene as the principal accessory minerals, it is probably pyroxene-rich gneiss formed under high grade metamorphism. These rocks occur in the extreme west-central part of the project area occupying about one-tenth ($^1/_{10}$) of its total areal extent. The rock unit is folded and steeply dipping to the east (60 – 80°) but gently dipping to the west (15 – 20″) with a plateau-like structure in the centre. The rock is dissected by seasonal streams. Most of the folds trend in a NE-SW direction.

#### 4.1.2.10 Sample 9

In hand specimen, the rock is fine-grained and equigranular, dark in colour (colour index 70-90), with mica flakes and feldspars clearly visible. The rock is unbanded and appears massive.

In thin section, the rock was examined under magnification of 32 and 100 (Appendix A8 – 10). The rock has the following major constituent minerals; quartz amphiboles (hornblende), Olivine, pyroxenes (augite), and biotite. The quartz are granular with defined subhedral faces, showing weak alignment along with other mafic minerals. There are also prismatic to roundish crystals of olivine, prismatic amphibole, fragments of pyroxene and platy foliated biotite mica. Most of the plagioclase feldspar crystals are also prismatic. The rock has the following modal composition by volume, %.

| | |
|---|---|
| Olivine | 15% |
| Pyroxene | 8% |
| Amphibole | 7% |
| Biotite | 10% |
| Plagioclase | 22% |
| Quartz | 35% |
| Accessories | 5% |

As the rock contains quartz, feldspars and foliated biotite, it is quartzofeldspathic, indicative of rocks of a granitic origin that must have undergone great changes possibly due to the rise in temperature and directed pressure. As it contains hornblende, prismatic plagioclase feldspars, quartz and biotite, it is an amphibolite, a basic metamorphic rock formed under medium grade conditions of regional metamorphism (Read, 1971). Deer *et al* (1978) and Olarewaju and Ajayi (1993) further assert that amphiboles are common constituents of regionally metamorphosed rocks and stable under wide range of pressure – temperature conditions. The amphibolites occur in four areas, two in the east-central part of the project area where it has been subjected to multiple faulting and folding; making contacts with simple pegmatitic granite to the east and west and hosts the Mayo Butale graphite. The third occurrence is in the south where it is characterized by steep dips in the northern-central end and gentle dips to the south. The fourth occurrence is south of Walon Kole village as a small outcrop where it has also been affected by tectonic forces involving faulting and block folding that trend NE-SW.

#### 4.1.2.11 Sample E

In hand specimen, the rock is light green coloured, coarse-grained, porphyritic, hollocrystalline (colour index 10-15). It has 2-3 cm megacrysts of orthoclase feldspars (Plate 18). Muscovite, biotite and quartz are clearly discernible to the unaided eye. Other minerals in the rock include sphene, magnetite, oligoclase, garnet, etc. This rock is exposed only along Mayo Nyanyare stream in the southern part of the project area. The approximate modal composition of the rock is as follows:-

| | |
|---|---|
| Quartz | 38% |
| Feldspars | 43% |
| Micas | 15% |
| Accessories (sphere, magnetite, oligoclease, garnet) | 4% |

The rock sample has been described in hand specimen only as it has not been analysed. Due to its constituent mineral assemblages however, the rock is plutonic, granitic and coarse-grained. It is muscovite-biotite granite (Plate 15). The modal compositions of rocks in the project area are summarized in Table 10 while Table 11 summarizes the thin section description of rocks from the project area.

Plate 15

**Table 10: Modal Composition (Vol. %) of Rocks from Toungo Project Area**

| Mineral type | Approximate Vol.% of mineral in the Rocks | | | | | | | | | | |
|---|---|---|---|---|---|---|---|---|---|---|---|
| Mineral type | 1A | 1B | 1C | 1D | 2A | 2B | 2C | 7 | 8 | 9 | E |
| Orthoclase feldspar | 14 | ___ | 14 | 28 | ___ | ___ | ___ | 10 | ___ | ___ | 14 |
| Plagioclase feldspar | 19 | ___ | 18 | 32 | 25 | 36 | ___ | 12 | 30 | 22 | 29 |
| Quartz | 33 | 51 | 41 | 28 | 15 | 12 | 44 | 47 | 32 | 35 | 38 |
| Microcline | 23 | ___ | ___ | ___ | ___ | ___ | ___ | ___ | ___ | ___ | |
| Biotite | 6 | 17 | 25 | 8 | 36 | 21 | 30 | 28 | 25 | 10 | 13 |
| Muscovite | 4 | 4 | ___ | ___ | ___ | ___ | 7 | ___ | ___ | ___ | 2 |
| Graphite | ___ | 26 | ___ | ___ | ___ | 9 | 14 | ___ | ___ | ___ | ___ |
| Pyroxene | ___ | ___ | ___ | ___ | 10 | 9 | ___ | ___ | 8 | 8 | ___ |
| Olivine | ___ | ___ | ___ | ___ | 9 | 7 | ___ | ___ | 4 | 15 | ___ |
| Amphibole | ___ | ___ | ___ | ___ | ___ | 11 | ___ | ___ | ___ | 7 | ___ |
| Garnet | ___ | ____ | ___ | 2 | ___ | ___ | ___ | 1 | ___ | ___ | ___ |
| Accessories | 1 | 2 | 2 | 2 | 5 | 4 | 5 | 2 | 1 | 5 | 2 |
| Total Groundmass | 100 | 100 | 100 | 100 | 100 | 100 | 100 | 100 | 100 | 100 | 100 |

Explanation

1A = Muscovite Biotite Granite

1B = Mayo Butale Graphite

1C = Medium grained Biotite Granite

1D = Simple granitic Pegmatite

2A = Migmatitic gneiss

2B = Migmatite

2C = Walon Kole Graphite

E = Coarse-grained, porphyritic biotite granite

7 = Granite gneiss

8 = Pyroxene gneiss

9 = Amphibolite

**Table 11 summarized thin section description of rocks from the project area**

| Slide no. | Magnification | Description | Polarization | Rock type |
|---|---|---|---|---|
| 1A | 32 | Altered orthoclase feldspar, quartz and biotite | Plane polars | Pegmatitic biotite granite |
| 1A | 32 | " | Cross polars | " |
| 1A | 10 | Orthoclase being altered to clay, biotite and anhedial quartz | Plane polars | " |
| 1A | 10 | " | Cross polars | " |
| 1A | 10 | Altered feldspar and anhedial quartz | Plane polars | " |
| 1A | 10 | " | Cross polars | " |
| 2C | 10 | Stretched quartz and aligned muscovite and graphite flakes | Plane polars | Graphite |
| 2C | 10 | " | Cross polars | Graphite |
| 1C | 3.2 | Anhedral quartz with undulose extinction, plagioclase feldspar and biotite flakes | Plane polars | Simple granitic pegmatite |
| 1C | | Anhedral quartz with undulose extinction, plagioclase feldspar and biotite flakes | Cross polars | " |
| 1D | 3.2 | Large microcline crystal to the top, anhedral quartz having vacuole exclusion and biotite | Plane polars | Biotite granite |
| 1D | 3.2 | " | Cross polars | " |
| 1D | 10 | Microcline, quartz and biotite | Plane polars | " |
| 1D | 10 | Plagioclase feldspar undergoing alteration to clay mineral | Cross polars | " |
| 2A | 10 | " | Cross polars | Migmatitic gneiss |
| 2A | 10 | " | Cross polars | " |
| 2A | 10 | Pyroxene and plagioclase feldspars | Cross polars | " |
| 2B | 3.2 | Prismatic plagioclase feldspar, olivine, pyroxene, biotite and quartz minerals. There are few dark inclusions on some of the minerals. | Plane polars | Migmatite |
| 2B | 3.2 | " | Cross polars | " |
| 2B | 10 | Olivine, pyroxene, plagioclase feldspar and quartz | Plane polars | " |
| 2B | 10 | " | Cross polars | " |
| 1B | 3.2 | Anhedral quartz with sutured boundaries enclosing muscovites and flakes of opaque mineral | Plane polars | Graphite |

| | | | | |
|---|---|---|---|---|
| | | (graphite). The muscovite shows alignment in a preferred direction | | |
| 1B | 3.2 | “ | Cross polars | “ |
| 2C | 10 | Quartz, muscovite and flakes of graphite | Plane polars | “ |
| 2C | 10 | “ | Cross polars | “ |
| 7 | 10 | Large quartz crystals with vacuole inclusions and biotite | Plane polars | Granite gneiss |
| 7 | 10 | “ | Cross polars | “ |
| 7 | 3.2 | Anhedral to sub-hedral quartz with lots of vacuole inclusion and deformed biotite | Plane polars | “ |
| 7 | 3.2 | “ | Cross polars | “ |
| 8 | 3.2 | Large pyroxene crystals, granular enhedral to sub-hedral quartz, plagioclase feldspar and biotite | Plane polars | Pyroxene gneiss |
| 8 | 3.2 | “ | Cross polars | “ |
| 8 | 10 | Pyroxene, plagioclase feldspar showing multiple twinning and quartz | Plane polars | “ |
| 8 | 10 | “ | Cross polars | “ |
| 9 | 3.2 | Euhedral to sub-hedral quartz crystals with mafic minerals most of which are prismatic amphibole, pyroxene, olivine and few biotite and fragments of plagioclase feldspars | Plane polars | Amphibolite |
| 9 | 3.2 | “ | Cross polars | “ |
| 9 | 10 | Olivine to the top right corner of the slide showing fractures, prismatic amphibole, pyroxene, biotite, quartz and feldspar | Plane polars | “ |
| 9 | 10 | “ | Cross polars | ” |

### 4.1.3 Physical, Metallurgical and Consumer Tests

**4.1.3.1 Physical Tests:** From the determinative tests conducted, the volume of the sample is given by Vol. = $W_2/d$ Where d = density of mercury at 24°C (which is given as 13.536gm/$cm^3$).

**a. Bulk Density:**

The bulk density of the specimen sample is obtained from the expression:

Bulk Density = $W_1d/W_2gm/cm^3$.

Table 14 shows the computed results of bulk density of Toungo graphite using Tecramics Densometer.

**b. Cold Crushing Strength**

The test results of cold crushing strength of Toungo graphite area is tabulated in Table 13. The cold crushing strength is given by CSS = M/A

Where M = mass in kg, and A = Area in $cm^2$

For graphite A: CCS = 430/6 = 71.66g/$cm^3$ and for graphite B: CCS = 360/6.25 = 57.60kg/$cm^3$

**a. Porosity**

Results of porosity tests conducted on the graphite samples and presented in Table 14 are computed using the formula: P = W – D/W – S x 100 (%)

Where W – D = Actual volume of the open pores of the graphite specimen

W – S = External volume of the graphite specimen

Computed values from Table 14 shows that the average apparent porosity of the graphite samples is 4.44% for sample from A (Walon Kole) and 7.51% for sample B (Mayo Butale).

**Table 12: Results of Bulk density of Toungo graphite**

| S/N | Sample | $W_1$ (g) | $W_2$ (gm) | B.Dg/$cm^3$ | Average |
|---|---|---|---|---|---|
| 1. | $A_1$ | 12.53 | 71.14 | 2.38 | 2.38 |
| 2. | $A_2$ | 12.12 | 68.87 | 2.38 | |
| 3. | $B_1$ | 9.37 | 53.70 | 2.36 | 2.29 |
| 4. | $B_2$ | 9.19 | 55.76 | 2.23 | |

A = Walon Kole sample; B = Mayo Butale sample

**Table 13: Computed results of cold crushing strength tests on Toungo graphite**

| Sample no | Length (cm) | Breadth (cm) | Area ($cm^2$) | Force applied (KN) | Mass (Kg) | C.C.S $(Kg/cm)^2$ |
|---|---|---|---|---|---|---|
| A | 3 | 2 | 6 | 4.3 | 430 | 71.67 |
| B | 2.5 | 2.5 | 6.25 | 3.6 | 360 | 57.60 |

A = Walon Kole sample; B = Mayo Butale sample

**Table 14: Results of apparent porosity of Toungo graphite**

| Sample no | D (g) | Wt of Container + $H_2O$ | Wt of Container + sample | S (g) | W (g) | A.P % | Average |
|---|---|---|---|---|---|---|---|
| A1 | 12.56 | 8.30 | 15.86 | 7.55 | 12.86 | 5.64 | |
| A2 | 12.25 | 8.24 | 15.60 | 7.35 | 12.42 | 3.25 | 4.44 |
| B1 | 9.24 | 8.24 | 13.98 | 5.62 | 9.68 | 8.14 | |
| B2 | 9.41 | 8.25 | 13.98 | 5.73 | 9.68 | 6.88 | 7.51 |

A = Walon Kole sample; B = Mayo Butale sample

### 4.1.3.2 Proximate Analysis Tests

Measurement for the various parameters (weight of sample, weight of residue, percentage of moisture content, volatile matter, ash content and fixed carbon) are given in Table 15.

**Table 15: Results of proximate analysis for Toungo graphite**

| S/N | Sample | Wt of sample (g) | Wt of residue (g) | Moisture content (%) | Volatile matter (%) | Ash content (%) | Fixed Carbon (%) |
|---|---|---|---|---|---|---|---|
| 1. | Walon Kole, graphite (A) | 1g | 0.96g | 0.27% | 2.10 | 96.1 | 1.53 |
| 2. | Mayo Butale (B) | 0.9g | 0.91g | 0.16 | 4.90 | 91.07 | 3.87 |

**a. Ash content**

From the formula expressed in section 3.2.3.2 and the measured parameters, the results of ash content for the Toungo graphite are given as follows:

| Measured Parameter | Samples | |
|---|---|---|
| | A | B |
| Weight of sample used (g) | 1 | 0.9 |
| Weight of residue (g) | 0.96 | 0.91 |

$$\text{Ash content for A} = \frac{0.96}{1} \times 100$$

$$= 96.1\%$$

Ash content for B = $\frac{0.91}{1}$ x 100

= 91.0%

Ash is generally considered to be the amount of inorganic mineral residue which cannot burn. Graphite is carbon in elemental form (that is, it is inorganic and not organic carbon), thus the amount of ash obtained invariably gives the amount of graphite in the sample. Hence, the high quality of the ash material denotes high quality graphite.

**b. Moisture content**

From section 3.2.3.2, the moisture content is given by

$\frac{\text{Difference in weight after heating}}{\text{Original weight of sample}}$ x 100

| | A | B |
|---|---|---|
| Weight of original sample | 1g | 1g |
| Weight after heating | 0.9973 | 0.9984 |
| Difference in weight after heating | 1 – 0.9973 | 1 – 0.9984 |
| Moisture content A = | 0.0027 | 0.0016 |

$$A = \frac{0.0027}{1 \times 100}$$

$$= 0.27$$

$$B = \frac{0.0016}{1 \times 100}$$

$$= 0.16$$

**c. Volatile matter**

From section 3.2.5.3, the volatile matter of the two graphite sample is given by

$$\text{Volatile matter} = \frac{\text{difference in weight after heating}}{\text{Weight of original sample}} \times 100$$

| | A | B |
|---|---|---|
| Weight of original sample | 1g | 1g |
| Weight after heating | 0.979 | 0.951 |
| Difference in wt after heating = | 0.021 | 0.049 |

Therefore, Volatile matter A = 0.021

$$A = \frac{0.0021}{1 \times 100} \qquad B = \frac{0.00491}{1 \times 100}$$

$$= 2.10\% \qquad = 4.90\%$$

**d. Fixed carbon**

From section 3.2.3.2, fixed carbon is determined from the results of ash content, volatile matter and moisture content of the sample

Fixed carbon == 100 – (%Vm + %Mc + %Ash)

Where % Vm, %Mc and %ash represents percent volatile matter, moisture content and ash content respectively. Therefore,

For graphite A, Fixed carbon = 100 – (2.10 + 0.27 + 96.10) = 1.53, and

graphite B, Fixed carbon = 100 – (4.9 + 0.16 + 91.07) = 3.87

### 4.1.3.3 Other Metallurgical Tests

**a. Specific Heat Capacity, Thermal and Electrical Conductivity**

Measurements of these parameters are given in Table 16.

**Table 16 Data on weights of tested graphite samples and range of temperatures of water and the environment during the test**

| S/N | PARAMETER | SAMPLE NO. | |
|---|---|---|---|
| | | A | B |
| 1. | Weight of sample | 12g | 14g |
| 2. | Temperature of environment | 26$^{o}$C | 26$^{o}$C |
| 3. | Temperature of cold water | 24$^{o}$C | 24$^{o}$C |
| 4. | Steady temperature of boiling water, upper $T_1$ | 89$^{o}$C | 80$^{o}$C |
| 5. | Steady temperature of boiling water, lower $T_2$ | 44$^{o}$C | 35$^{o}$C |

The specific heat capacity of the graphite samples can be read off from the graph (Fig 21). For sample A, the value is given as $3.8 \times 10^3$ $JK^{-1}$ $C^{-1}$ and for B, it is $0.227 \pm 820 \times 10^{-3}$ $JK^{-1}$ $C^{-1}$ (Fig. 22). The thermal conductivity (i.e. the heat passing through a square centimeter in one second) is deduced from Figures 23 and 24. It is given by the relation;

$$\text{Thermal conductivity} = \frac{\text{Heat/square/sec}}{\text{Temp.gradient}}$$

From the graph (Fig 23), thermal conductivity K for sample A is found to be $1.26 \times 10^4$ J/Kg. As electrical resistivity is inversely proportional to the thermal conductivity, K

Electrical Resistivity = 1/K

$= 1/1.26 \times 10^4$ $JK^{-1}gk^{-1}$

Therefore, Electrical Resistivity = 7.93 x 10-5 ΩM (Ohm - meter).

For sample B, the thermal conductivity is $1.9 \times 10^4$ J/Kg K (Fig. 24). Therefore, the Electrical Resistivity, E = 1/K

$= 1/1.9 \times 10^4$

$= 5.26 \times 10^{-5}$ ΩM (Ohm - meter)

**b. Test results for compressive strength**

Results for compressive strength test for Toungo graphite are given in Table 17

Using the formula $T_c = P_{max} / A_o$

Fig 20

Fig 21

Fig 22

Fig 23

Where $T_c$ = compressive strength

$P_{max}$ = maximum load applied and, $A_o$ = Area of sample

The compressive strength for the two samples is:

For sample A, Walon Kole graphite,

$T_c$ = 1380/60 = 23N/mm$^2$ and for

Sample B, Mayo Butale graphite

$T_c$ = 990/60 = 16.5N/mm$^2$

**Table 17: Test results for compressive strength of Toungo graphite**

| Sample no. | Area of sample | Load applied (Newtons, N) | | | | | |
|---|---|---|---|---|---|---|---|
| A | 60mm$^2$ | 100 | 200 | 400 | 800 | 1200 | 1380 |
| B | 60mm$^2$ | 100 | 200 | 400 | 800 | 990 | |
| Time interval | | 0 | 2 | 4 | 8 | 12 | 15 |

## 4.2 DISCUSSION OF THE RESULTS

Toungo area is underlain by migmatite-gneiss-quartzite complex of the Nigerian Basement Complex rocks which have sequentially been invaded by the Pan African granites during the Pan African thermo tectonic period.

Field and laboratory studies indicate the rocks in the area were subjected to a wide range of tectonic disturbances involving fracturing, faulting, shearing, granitization and metamorphism. These are evidenced by the different structures discovered during the course of this project, typical of which are microfaults, jointing infilled with veins, block-faulting and folding, shearing, subsidence mega folding and faulting. The orientations of these structures are

mainly NE – SW, and SW – NE in consonance with the Pan African orogeny (McCury, 1976; Dada, 1981; Rahaman, 2003). The oldest rocks in the area are fine to medium to coarse grained, foliated and characterized by quartz-feldspathic veins which is indicative of deformation brought about by tectonic stresses.

The massive melanocratic amphibolite (MMA) variety (Rahaman *et al*, 1988) is the main amphibolite variety in the area. Quartz, plagioclase feldspars, biotite, pyroxene, olivine and amphibole are the principal constituent minerals forming the amphibolites in these areas. These mineral assemblages portray the amphibolites as formed in highest grade of amphibolites facies metamorphism (Bard, 1983, Ephraim, 2009a).

Studies by Bard (1970) and Olarewajiu and Ajayi (1993) show that the MMA amphibolite varieties with Al values in the range of 0.7 to 0.9 and higher than 0.5 for high grade stripped amphibolites and garnet amphibolites are characteristics of rocks from areas of high load pressure, indicating that MMA amphibolites could be subjected to this range of pressure during metamorphism. Values of 3.74 obtained for Toungo amphibolites are therefore indicative of environment of high grade metamorphism, possibly upper amphibolite facies metamorphism and granulite facies metamorphism. These are shown by stresses and chemical variation diagrams especially by the Differentiation Index (DI) plots (Fig. 16), which show two major evolutionary trends for rocks of the area. The first trend is shown by a, b, c, e, g and k in which DI values decrease with increasing elemental values, while the second trend is shown by d, f, h, i, l, m and n where DI values increase with increasing elemental values. The amphibolites are lesser in $Na_2O$, $SiO_2$, $P_2O_5$ and MnO but richer in $TiO_2$, $Al_2O_3$, $Fe_2O_3$, CaO and $K_2O$; $K_2O/Na_2O$ ratio is low but high values are recorded for $TiO_2/Al_2O_3$ and $Al_2O_3/Na_2O$ as shown on Table 9.

Major element concentrations (oxides) of the two major rock types in the area are given in Table 9, while Table 18 shows comparison of the major element oxides with similar rocks elsewhere. Possible increase in MgO with increasing $SiO_2$ for the alkaline (acidic) rocks implies fractional crystallization from an igneous melt (Ukwang and Ekwueme, 2009). This is further evidenced by the oxide ratio $K_2O/Na_2O > 1$ and $K_2O > Na_2O$ for the rock (Table 9), indicating an igneous nature of the melts. The linear geochemical variations shown by Harker plots and chemical variation diagrams (Figs. 17 and 19) are indicative of the genetic relationships between the rocks; an indication of possible fractional crystallization during formation from mixed sources. Most of the rocks correlate with $SiO_2$ as shown by $Na_2O$, MgO, CaO and $Fe_2O_3$. However, $K_2O$, $TiO_2$ and MnO have weak correlations as they show scatter plots (Harker plots) due to possible accumulation of various components and mixtures during fractional crystallization.

The field and laboratory studies confirm that the area forms part of the Nigerian Precambrian basement and the Adamawa Massif, one of the principal components of the Cameroun volcanic line. The orientation of the structures from the area (Fig 14) is a possible indication of a polyphase deformation similar to those of the Oban Massif, Obudu Plateau (Ukwang and Ekwueme, 2009) which also form part of the Cameroun line. The tectonic in the structures in Fig. 14 trend mostly NE – SW and subordinately SW – NE. These trends form the most wide spread deformation structures which occurred during the Pan African thermotectonic events in the Nigerian basement, (McCurry and Wright 1971; Rahaman *et al*, 1983).

**TABLE 18 COMPARISON OF MAJOR ELEMENTAL COMPONENTS OF ROCKS IN THE PROJECT AREA AND SIMILAR ROCKS FROM OTHER PLACES**

| Lithology | 1 | 2 | 3 | 4 | 5 | 6 | 7 | 8 | 9 | 10 |
|---|---|---|---|---|---|---|---|---|---|---|
| $SiO_2$ | 44.73 | 52.11 | 50.00 | 52.97 | 64.02 | 63.02 | 46.23 | 50.31 | 73.74 | 51.20 |
| $TiO_2$ | 0.18 | 1.23 | 2.33 | 1.40 | 0.65 | 0.96 | 0.57 | 0.47 | 0.20 | 0.77 |
| $Al_2O_3$ | 15.86 | 16.86 | 13.10 | 14.76 | 15.82 | 16.26 | 16.78 | 14.31 | 12.92 | 14.78 |
| $Fe_2O_3$ | 2.10 | 7.95 | 2.12 | 13.06 | 5.05 | 6.50 | 1.99 | 2.17 | 0.49 | 2.81 |
| FeO | 2.26 | 8.02 | 9.58 | – | – | – | 0.63 | 6.58 | 2.26 | 8.43 |
| MnO | 0.38 | 0.35 | 0.15 | 0.22 | 0.08 | 0.006 | 0.19 | 0.16 | 0.06 | 0.21 |
| MgO | 3.78 | 7.80 | 7.42 | 4.02 | 2.56 | 1.98 | 9.46 | 10.62 | 1.08 | 6.25 |
| CaO | 3.78 | 7.80 | 8.60 | 5.83 | 3.74 | 3.37 | 13.26 | 10.62 | 0.60 | 8.06 |
| $Na_2O$ | 0.42 | 0.79 | 3.34 | 5.04 | 3.06 | 3.15 | 1.85 | 2.58 | 3.39 | 2.12 |
| $K_2O$ | 33.55 | 16.69 | 0.77 | 0.35 | 2.21 | 3.35 | 1.87 | 2.46 | 2.72 | 1.06 |
| $P_2O_5$ | 0.80 | 0.79 | 0.26 | 0.16 | 0.47 | 0.45 | 0.20 | 0.25 | 0.04 | 0.21 |
| L.O.I | – | – | 1.72 | – | – | 0.75 | – | – | 1.47 | 1.54 |
| $H_2O$ | – | – | – | 1.94 | 1.06 | – | – | – | – | – |
| **TOTAL** | **101.25** | **102.08** | **99.40** | **99.74** | **98.79** | **99.80** | **100.41** | **100.00** | **98.04** | **98.90** |

Key:

1. Migmatite gneiss, Toungo, present work
2. Muscovite Biotite granite, Toungo, present work
3. Unmetamorphosed mafic dyke in Precambrian basement of south-east Nigeria (Ekwueme, 1990).
4. Amphibolite, northern Cameroun, (Toteu, 1990)
5. Gneisses, northern Cameroun, (Toteu, 1990)
6. Migmatitic rocks of Obudu, Nigeria (Ephraim, 2009b)
7. Marangudzi dyke rocks, Zimbabwe (Ezepue and Henderson, 1990)
8. Marandudzi dyke rocks, Zimbabwe (Ezepue and Henderson, 1990)
9. Quartz-feldspar gneiss from high grade metamorphic terrain, Saxberget, Sweden (Vivallo and Rickard, 1990).
10. Amphibolite from high grade metamorphic terrain, Saxberget, Sweden (Vivallo and Rickard, 1990).

The influence of $CO_2$ infiltration on graphite formations in the area could best be explained by the reaction

$$C + H_2O \longrightarrow CO + H_2$$

$$2CO \xrightarrow{heat} C + CO_2$$

Carbon is present in all rocks, but it can however be depleted from some rocks by migration of $CO_2$-rich fluids (Gautneb and Tveten 2000). The influence of $CO_2$ infiltration on graphite formation can best be explained by the fact that the $CO_2$-rich fluids were depleted by migration of the fluids from originally rich graphitic rocks (1A, 1C, 1D, 2A, 2B, 7, 8 and 9) to negative values (Appendix 2). It can also be seen from the geological map of the area as the rocks immediately bordering the graphite zone are less depleted. Depletion or decay is more pronounced in rocks further away from the graphite zone. This is further evidenced by the high quartz and feldspar contents of the rocks and by values of the chemical composition of the rocks ($SiO_2$ for 1A, 1C and 1D are 2.11, 33.58 and 80.42 respectively). The migration might have been caused by changes in temperature, pressure, pH, oxidation state and other chemical disturbances during granitization (Nockolds *et al*, 1979).

The results obtained from the investigation of two different graphitic rocks have been presented (in section 4.1) in terms of physical and chemical parameters. The fundamental assumptions inherent in these test methods are that the samples are representative of the material in general and the particle size of the sample were within the range specification by the test method. Bulk density and porosity are properties that characterize the quality or consistency of quality of granular refractory material when determining its suitability for usage. These test methods can be used as quality control tests in the manufacture or mining of refractory raw materials. These test methods are primary standard methods and thus are suitable for use in

specifications, quality control, and research and development. They can also serve as a reference test methods in purchasing controls or agreement. From the result obtained in the investigation, sample 2C (Walon Kole graphite) has a value very close to the standard bulk density for graphite. The observed difference between the deposits gave an indication that sample 2C is of higher purity than sample 1B (Mayo Butale). The difference between the standard value and that of sample 2C and sample 1B reasonably confirm the raw nature of the material under investigation. The porosity results obtained also suggest that the two samples investigated are not porous materials. High porosity values can be detrimental to such properties like heat conductivity and strength, thus making it unsuitable for some applications. The compressive strength test provides a measure of the maximum load bearing capability of carbon or graphite material. The compressive strengths obtained from this investigation are low an indication that strength test is carried on formed graphite and not the raw material. Flexural strength is a measure of the ultimate load carrying capacity of a specified beam in bending and is usually conducted on manufactured component using a simple beam in four points loading at room temperature. The microstructural analysis carried out on the sample revealed short lamellae flakes while the chemical inertness of the sample was manifested due to its non-reaction when etched in solution of 4% $HNO_3$ in methylated spirit.

The thermal shock resistances (in section 3.2.3.3 – C) are highly satisfactory for the two samples under investigation as they withstood severe cycles without failure; an indication of high thermal shock that is quite higher than some known commercial refractories. The thermal conductivity of carbon refractories is a property required for selecting their thermal transmission characteristics. The data from this test method is suitable for specification acceptance, estimating

heat loss and surface temperature and the design of multi-layer refractory construction. The result obtained from this investigation is contained in Figs. 22 – 23 and Appendices 2 (a and b).

The electrical resistivity is a property of a material that determines its resistance to the flow of an electrical current. The test specimen may be in the form of a strip, rod bar or tube (Fig. 13). The result obtained for this parameter is also given in Figs. 22 and 23 and in Appendix 4a and 4b. The data obtained in all the investigations are quite satisfactory and in most cases very close to the standard obtained for processed graphite. The data obtained can be enhanced through upgrading (Tatas, 2008) and mechanically formed into structural components for application requiring high thermal stability as demanded during service applications like metallurgical processes.

The light weight as demonstrated by the bulk density parameter together with the low thermal expansion makes the material less susceptibility to crushing, cracking and spaking. The material particularly sample 2C (Walon Kole), when carefully processed can be impregnated with chemically resistant resins without imparing the thermal conductivity of the base material. By this arrangement, the material can be rendered impervious to fluids under pressure and the strength can also be increased thereby rendering it utilizable in practically all chemical conditions in which the base materials are resistant (Klett, 1998; Klett and Stouder, 2005a).

The high electrical resistivity and thermal conductivity confer a high thermal shock to the material and can be used to advantage in electrical fields and in allied industries such as aerospace applications. Its chemical inertness as demonstrated by its non-reaction with 4% Nitric acid ($HNO_3$) in methylated spirit can also be used to advantage in a corrosive environment. The resin impregnated graphite can be produced into structural components such as beams, plates

(Klett and Stouder, 2005(b) files and rods and used as construction materials where corrosive chemicals and severe thermal shock conditions are encountered. The beam could be used as supporting members in tanks or vessels in chemical plants and paper mills.

# CHAPTER FIVE

## SUMMARY, CONCLUSION AND RECOMMENDATION

Detailed field investigations and laboratory studies have been undertaken on the crystalline flake graphite deposits which occur within the Precambrian Basement Complex rocks of Toungo area of Adamawa State. The studies were carried out in order to assess the potentialities of the deposits for possible industrial utilization. The geological investigation indicates that the deposits are hosted by metamorphosed rocks, essentially amphibolites, associated with migmatitic-gneiss and Pan African granites.

The laboratory investigations involved chemical and determinative studies and were carried out in Nigeria as well as in the United Kingdom. Results of the investigations have been presented, synthesized and interpreted. The results of chemical, metallurgical and consumer tests carried out on Toungo graphite conform to international quality standards for industrial utilization.

From the combined lines of evidence obtained from the field investigations, physical, chemical and metallurgical characteristics of Toungo graphite, it can be concluded as follows:

1. That Toungo area is underlain by the Precambrian Basement Complex rocks similar to other basement rocks in Nigeria.
2. That these rocks evolved through progressive regional metamorphism, granite intrusions through tectonic episodes of geology.

3. That the area was subjected to orogenesis during the Pan African orogeny which involved uplift, cooling, fracturing, faulting and high level magmatic activity which gave rise to the emplacement of Pan African granites in the area.
4. That the quality of the graphite in the area can be upgraded to meet the required industrial standards based on its physical, chemical and metallurgical characteristics.

On the basis of the foregoing, it is recommended that:

1. Viability awareness on the numerous uses of this strategic mineral in industries should be conducted by Government agencies, professionals and academicians, researchers and consultants.
2. Follow-up studies such as detailed feasibility studies should be undertaken by Government or indigenous/multinational mining companies in order to explore the graphite in the area and its environs.

## REFERENCES


ADEBAYO, A.A. and TUKUR A.L., (Eds), 1999: Adamawa State in maps – Paraclete Publishers, Yola. 112 p

ADEGOKE, O.S., ADEDIRAN, S.A. and ELUEZE, A.A. (eds), 1989: Non-metallic Mineral Multidisciplinary Taskforce, 1989: Guide to the non-metallic Mineral Industrial Potentials of Nigeria, 1989, Raw Material Research and Development Council, 1989.

AHMED, F. and ALMOND, D.C. 1983; Field Mapping for Geology students, George Allen and Unwin Ltd, 72 p

BACOS M.P., (1993); Carbon-Carbon Composites: Oxidation Behaviours and coatings Protection, in Journal de Physique IV Collique C7, supplement au Journal de physique III, volume 3, Nov. 1993, p. 1895 – 1903

BAKER R.T.K., 1998: Synthesis, Properties and applications of graphite nanofibers, http://www.wtec.org/loyola/nano/us_r_n_d/09_03.htm

BARD, J.P., 1970: Hornblende formed during Hercynian progressive metamorphism of the Aracena metamorphic belt, S.W. Spain. Contr. Miner. Petr, 28; p. 117 – 134

BARD, J.P., 1983: Metamorphic evolution of an obducted island Arc; example of Kohistan sequence, (Pakistan) in the Himalayan collided range, Geological Bulletin, Peshawor, 161 p. 105 – 184

BILLINGS, M.P., 1972: Structural Geology – Printice-Hall Inc., 606 p

BOYLAN T., (1996); Structure of Carbon-Carbon Composites and Carbon-Graphite in: Material World vol.4 no. 12, p 707 – 708

BRIQUIER L. DADA, S.S, DUPRE, B. and RAHAMAN, M.A., 1994: Geochemical Characteristics of reworked Archean gneiss complex of north-central Nigeria: 30th Annual Conference of Nigeria Mining and Geoscience Society (NMGS), Jos, Nigeria, Abstract vol. 65

CERAMISIS Graphite, 2010: High density carbon and graphite materials specifications; Adapted from http://www.ceramisis.com/carbongraphitea1.htm,2010

CERAM RESEARCH, (2006): http://www.azon.com/details.sap?Article1D/630

CONSULINT (NIG) LTD, (1976): Water Survey of the North-Eastern State – General report, vol. 2, (Hydrogeology) p. 16 – 110

CONSULINT (NIG) LTD, (1976): Water Survey of the Northeastern state, Gen. report, vol. 4 (Geology), p. 50 – 61

COURSEY J.S., KIM J., and BOURDEAUX P.J., (2005); Performance of Graphite Foam Evaporator for Use in Thermal Management, Journal of Electronic Packing, vol. 127, 6/2005, p. 127 – 134

DADA O., (1981): The Schist Belt of the Nigerian Precambrian and its Potentials for Raw Material Development for Steel Plants in Nigeria, in: Precambrian Geology of Nigeria, GSN, 1981, p. 211 – 227

DADA, S.S., TUBOSON I.A., LANCELOT, J.R, and LAU, A.U., 1993: Late Archean u-pb age for the reactivated basement of northeastern Nigeria. Journal of African Earth Science, vol. 16, p. 405 – 412

DAR-AL HANDASAH and PARTNERS, 1978: Govt. of Gongola State, MOWLS Preliminary Master Plan, Gongola State, 1977 – 2000; sec, 1.1, 1.2

DEER, W.A., HOWIE, R.A., and ZUSSMAN, J., 1978: An introduction to the rock-forming minerals – English Language Book Society and Longman, 528 p

DEPARTMENT OF MINING ENGINNERING, Osmangazi University, Eskisehir, Turkey (2005); Beneficiation of Graphite from Moulding Factory Wastes, http://www.ncbi.nlm.nih.gov/pubmed/16200984

EKWUEME, B.N., (1990): Mafic dykes in the Precambrian Basement of southeastern Nigeria, In: Mafic Dykes and Emplacement Mechanism, Parker Ringwood and Tucker (eds) Balkema Rotterdam, p. 245 – 309

EKWUEME, B.N., (2003): The Precambrian Geology and Evolution of the South Eastern Nigerian Basement Complex, University of Calabar, Press, 2003, 135 p

EKWUEME, B.N, and KRONER, A; (1997): Zircon evaporation ages and chemical composition of migmatitic schist in the Obudu Plateau in evidence for palae proterozoic (Ca. 1789) components in the Basement complex of Southeastern Nigeria, Journal of Mining and Geology, vol. 33 (2) p. 81 – 88

EKWUEME, B.N, and KRONER, A; 2000: Single Zircon evaporation ages from Obudu Plateau; first evidence of Archean components in the schists of Southeastern Nigeria in

the 36th Annual Conference of Nigerian Mining and Geoscience Society (NMGS), Enugu, Nigeria, vol. 2, Abstract, 14 p

ELERT, G., (2004): Resistivity of Carbon and Graphite, Africa Belgrave published by http://www.hypertextbook.com/facts/2004/AfricaBelgrave.shtml-Resistivityofcarbongraphite

EPHRAIM, B.E., 2009a; Compositional Features and Petrogenetic Characteristics of Migmatic Rocks of Northeast Obudu Basement Massif, Southeastern Nigeria, Journal of Mining and Geology, vol. 45 (1), 2009, p. 1 – 11

EPHRAIM, B.E., 2009b: Petrochemistry and Petrogenesis of granite gneiss of Northeast Obudu Basement Massif, southeastern Nigeria, Journal of Mining and Geology, vol. 45 (2), 2009, p. 59 – 71

EZEPUE, M.C. and HENDERSON, C.M.B., (1990): Geochemistry of dyke rocks from Marangudzi igneous complex, Zimbabwe, Journal of Mining and Geology, vol. 26 (1), 1990, p. 55 – 68

GARBA I., (2002); geochemical characteristics of the gold mineralization near Tsohon Birnin Gwari, Northwestern Nigeria, IN: Chemical der ERDE Geochemistry 62, (2000) p. 160 – 170.

GAUTNEB H., and TVETEN E., (2008); The Geology, Exploration and Charaterization of graphite deposit in the Jennestard area, Vesteralen, Northern Norway, Norges Geologiske undersokelse Bulletin 436, p. 67 – 74, Published in Google under file http://www.ngu.no/fileArchive/102/Bulletin436_7pdf

GEOLOGICAL SURVEY OF NIGERIA (GSN) 1987: Minerals and Industry in Nigeria, GSN 1987, 60 p

GRANT, N.T., 1969: The late Precambrian to early Paleozoic Pan African orogeny in Ghana, Togo, Dahomey and Nigeria, Geological Society of America, Bulletin 80, p. 45 - 56

HOBBS, B.E., MEANS W.D. and WILLIAMS, P.F., 1976: An Outline of structural Geology, John Wiley and Sons; 481 p

HURLBUT C.S., and KLEIN C., (1971): Manual of Mineralogy (After J.D., Dana) John Willey and Sons, 1971 536 p

IRVINE, T.N and BARAGAR, W.R.A; 1971: A guide to the chemical classification of common volcanic rocks in: Canadian Journal of Earth Science, vol 8, p. 523 – 548

KINDLER A.E., (1983): Oxidation Resistance of Industrial Carbon and Graphite Grades, 16th Biennial Conference on Carbon at San Diego, 1983

KLETT J., (1998): High Thermal Conductivity Mesophase – Derived Carbon foam; http://www.ms.ornl.gov/cimtech/cimtech.html

KLETT J., (2002); High Thermal Conductivity Graphite Foams for Compact Lightweight Radiators, http://www.ms.ornl.gov/sections/mpst/cimtech/default.html

KLETT J., and KAUFMAN J., (2005); Graphite Foam Helps Keep Soldiers Cool – Microclimate Cooling, US Dept. of Energy, Energy Efficiency and Renewable Energy Program

KLETT J., and LEICHT B., (2005)(a): Graphite Foam enables New Space Technologies; Space Radiators. US Dept. of Energy, Energy Efficiency and Renewable Energy Program, http://www.skyrocket.de/space/doc_sdat/xss-11.htm

KLETT J., and LEICHT B., (2005)(b): Graphite Foam helps Computers Run Faster – Evaporative Cooling; US Dept. of Energy, Energy Efficiency and Renewable Energy Program, http://www.skyrocket.de/space/doc_sdat/xss-11.htm

KLETT J., and STOUDER R., (2005)(a); High Thermal Conductivity Graphite Foams – Lightweight materials, US Dept. of Energy, Energy Efficiency and Renewable Energy Program, http://www.pocofoam.com

KLETT J., and STOUDER R., (2005)(b); Graphite Foam Enables Lightweight Cold Plates – Thermal Sinks, US Dept. of Energy, Energy Efficiency and Renewable Energy Program

KLETT J., MCMILLAN A., GALLEGO N., and WALLS, C (1998); The Role of Structure on the Thermal Properties of Graphitic Foams, http://www.thirdwave.de/3w/tech/mnt/cfoamstructure.pdf

LAKIN J.R., (1997); Assessment Techniques for Graphite Electrodes; In: Proceedings of the Conference on Tar Pitch, Solvent-refined Coal and Petroleum as used in Carbon and Graphite Production, 1977 – Society of Chemical Industry, UK,

http://www.sciencedirect.com/science/article/pii/0016236178900674 Assessment techniques for graphite electrodesstar, open

LEE W.S., and LEE J.K., (2009); Graphene Hybrid Material and Method for preparing same using Chemical Vapour Deposition, http://www.fags.org/patents/app/20090047520

LUEKING A.D., PAN L., KARAYANAN D.L., and CLIFFORD C.B., (2005); Exfoliated Graphite nanofibers for hydrogen Storage

LUQUE, F.J; PASTERIS, J.D., WOPENKA, B. and BARRENCHEA J.F., 1998: Natural fluid deposited graphite; Mineralogical characteristics and Mechanisms of formation, American Journal of Science, vol. 298, June 1998 421 – 498 p

LU W., and CHUNG D.D.L., (2002); Oxidation Protection of Carbon Materials by acid Phosphate impregnation in; Carbon 40 (2002), p 1249 – 1254

LUO, X., CHUGH R., BILLER B.C., HOI Y.M., and CHUNG D.D.L., (2002); Electronic Applications of Flexible Graphite in; Journal of Electronic Materials vol. 31, no. 5, 2002

MARSDEN B.J., (2010); Stresses and Deformations in Graphite Bricks, http://www.web.up.ac.za/sitefiles/file/44/2063

McCURRY, P., and WRIGHT, J.B., 1971; On Place and Time in Orogenic Granite Plutonisan; Geological Society of America Bulletin, Vol. 82, p. 1713 – 1716

McCURRY, P., 1976: A general Review of the Geology of the Precambrian to lower Paleozoic rocks of the Northern Nigeria, IN: Geology of Nigeria, Kogbe, (Ed), pp. 13 – 37

MICROSOFT ENCARTA 2009: © Application of Graphite, Microsoft Encarta ® 2009 Microsoft Corporation. All rights reserved

MICROSOFT ENCARTA, 2010: Nuclear Energy, Microsoft Encarta ® 2009 Microsoft Corporation. All rights reserved

MINISTRY OF COMMERCE, INDUSTRIES AND SOLID MINERALS DEVELOPMENT, YOLA (2004): Reconnaissance Geological and Mineral Resources Surveys Report, vol. 1, Southern Adamawa, 28 p

MIROSHNIKOV V.N., and DENISENKO E.T., (1964); Assessment of the Feasibility of operation of Nickel-Graphite Composition in Steam at Atmospheres in Industrial Parameters, Poroshkovaya Metallurgies, no. 6 (24)

MITCHELL, C.J., (1993): Industrial Minerals Laboratory Manual, British Geological Surveys, Technical Report no. WG/92/30_Mineralogy and Petrology

NATIONAL POPULATION COMMISSION, Adamawa State Office, 2011: 2006 Population Census, Final Figures, Adamawa State.

NOCKOLDS, S.R., and ALLEN, R; 1953; The Geochemistry of some igneous rock series, Geochimcosmochim Acta, vol. 4, 105 – 142 p

NOCKOLDS, S.R., KNOX, R.W. and CHINNER G.A., 1979: Petrology for students, Cambridge Uni. Press 435 p

NWANEBI N.M.E., (2000); Windows of Opportunities in Nigeria - Nigeria on a Shoe String, Etmmco Ltd, 2000, 151 p

NWOBI B.E., AHMED A.S., and ADEREMI B.O., 2002; Beneficiation and Characterization of Bauchi Graphite, Unpublished M.Sc Thesis, ABU Zaria

OGEZI, A.E., 1996: Thesis and Technical Reports in Geology and Related Fields, Ministry of Solid Minerals Dev., Geological Survey of Nigeria, Training Manual Series.

OLAREWAJU V.O. and AJAYI, T.R., 1993: Microprobe Studies of main ferromagnesian minerals in the amphibolites of Ife-Ilesa schist belt, Southwest Nigeria, IN: Journal of Mining and Geology, vol. 29, no. 1993, p. 59 - 69

OLSON, D. W., (2009); Graphite, Advance Release, US Dept. of The Interior and US Geological Survey, 2011, http://www.pubs.usgs.gov/ds/2005/1401

PARK C., Tan C.D., HIDALGO, BAKER R.T.K., and RODINGUEZ N.M., (1997); Hydrogen Storage in Graphite Nanofibers in: Proceedings of the 1998 US DOE Hydrogen Program Review Publication no. NREL/CP-570-25315

PERFORMANCE COMPOSITES, (2010); Graphite Composites Material Design Guide, http://www.performancecomposites.com/graphitedesignguide.pdf

PIHURA D., and ORUC M., (2007); The Application of Spheroidal Graphite Cast Iron in Bosnia and Herzegovina; Materials and Technology, 4/(2007), 4, p. 193 – 195

PYROTEK, (2008); Graphite Products and Specializations, Pyrotek Int. http://www.pyrotek.info/locations

RAHAMAN M.A, 1981: Recent advances in the study of Basement Complex Nigeria, First Symposium on Precambrian Geology of Nigeria (11 - 43) GSN pub.

RAHAMAN, M.A., (2003): An address delivered by president, NMGS at the Annual International Conference, Itakpe, IN: The Crust Vol. 26, no. 2

RAHAMAN, M.A., AJAYI I.R., OSHIN I.O., and ASUBIOJO, I.O.I, (1988): Trace element geochemistry in geotectonic setting of Ife - Ilesa schist belt, IN: Precambrian Geology of Nigeria, vol. 1, p. 241 – 256

RAHAMAN, M.A., EMOFURIETA, W.O., and CAEN VACHETTE, M., 1983: The potassic granites of the polycyclic evolution of the Pan African belt in Southwestern Nigeria, Precambrian Resources, vol. 22, p. 75 – 92

READ, H.H., (1971): Rutley's Elements of Mineraology-Thomas Murphy and Co. London, 560p

REVILOCK J.F., (1990); "Grafoil" Graphite Tape – its Manufacture, Properties and Uses; http://www.anl.gov

ROBERTS, R.G. and SHEAHAN, P.A., (eds) 1990: Ore Deposits Models, Geoscience Canada, Reprints series 3, 181 p

ROLLINSON, H.G., 1993: using Geochemical Data Evaluation. Presentation and Interpretation; Longman and John Wiley, 352 p

SCHUNK KOHLENSTOFFTECHNIK GMBH, (2004); Manufacturing, Processing and Material Properties of Carbon and Graphite Materials, http://www.schunk-group.com

SIMANDI G.J., and KENAN, W.M., (1997): Crystalline Flake Graphite, IN: Geological Field work, British Columbia, Ministry of Employment and Investment, paper 1998 – 1, pp. 2x p-1, 24 p.3, http://www.emgov.bc.ca/mining/geo/survey/metalliferousminerals/mineraldepositprofiles/profiles/PO4.htm

SUPERIOR GRAPHITE, (2006); Graphite Industrial Assessment, US Dept. of Energy, Industrial Technologies and Program, http://www.eere.energy.gov/industry

TATAS, T.T., (2008); Beneficiation and Characterization of Adamawa Graphite, Unpublished M.Sc Thesis, Federal University of Technology, Yola, 2008

TOTEU, S.F., 1990: Geochemical characteristics of the main Petrographical and Structural Units of Northern Cameroun: Implications for Pan African Evolution, IN: Journal of African Earth Science, vol. 10, no. 4, p. 615 – 624

UKWANG, E. and EKWUEME, B.N., 2009: Geochemistry and geotectonic study of granitic rocks, southwest Obudu, Plateau, southwestern Nigeria, IN: Journal of Mining and Geology, vol. 45 no. 2, p. 73 – 82

VIVALLO, W. and RICKARD, D., 1990: Genesis of an Early Proterozoic Zinc Deposits in High-Grade Metamorphic Terrain, Saxberget, Central Sweden, IN: Economic Geology, vol. 85, 1990, p. 714 - 736

WALKER T.B., and BOOKER L.A., 2001; Oxidation Protection for Carbon/Carbon Composites and Graphites, US Patent and Trade Mark Office, Publication no Wo/2001/060763, 2001

WASTE MANAGEMENT RESOURCES., 1995: Beneficiation of flake graphite US patent application no. 08/417707, Dec., 1995 – published by htt://www.sagepub.com/content/23/4/338, abstract

WEYMAN, 1981: Tectonic Stresses; George Allen and Unwin, London, 102 p

WIKIPEDIA, the Free Encyclopedia, (2008); Graphite, http://www.wikipedia.org

WIKIPEDIA, the Free Encyclopedia, (2010); Amphibolite, http://www.wikipedia.org

WIKIPEDIA, the Free Encyclopedia, (2011a); Graphene, http://www.wikipedia.org

Wikipedia, the Free Encyclopedia, (2011b); Carbon and Graphite Felts; Industrial applications, http://www.wikipedia.org

WOAKES, M., RAHAMAN, M.A., and AJIBADE, A.C., 1987: Some metallogenic features of the Nigerian Basement, IN: Journal of African Earth Sciences, vo. 6, no. 5, p. 655 – 664.